The Thesis Committee for Grant Zheng

Certifies that this is the approved version of the following thesis:

Control of high precision roll-to-roll manufacturing systems

APPROVED BY

SUPERVISING COMMITTEE:

Dongmei Chen, Supervisor

Mitchell Pryor

Control of high precision roll-to-roll manufacturing systems

by

Grant Zheng

Thesis

Presented to the Faculty of the Graduate School of

The University of Texas at Austin

in Partial Fulfillment

of the Requirements

for the Degree of

Master of Science in Engineering

The University of Texas at Austin

December 2018

Acknowledgements

I would like to thank my advisor Dr. Dongmei Chen for her support throughout my graduate studies. Without her support, I would not have overcome many of the challenges I faced in the past two years, both academically and professionally.

I would also like to thank Dr. Mitchell Pryor for showing me the fundamentals of control theory and giving his time and assistance as a second reader for this thesis.

I also want to thank my classmates and lab mates in Dr. Chen's group. My peers have been instrumental in my understanding of engineering through coursework and research.

Finally, I would like to thank all my friends and family members for their support and patience

Abstract

Control of high precision roll-to-roll manufacturing systems

Grant Zheng, M.S.E.
The University of Texas at Austin, 2018

Supervisor: Dongmei Chen

The flexible electronic industry has been growing rapidly over the past decade. One of the barriers to commercialization is the high cost of manufacturing micro- and nano-scale printed electronics using traditional methods. Roll-to-roll manufacturing has been identified as a method of achieving low cost and high throughput.

A dynamic model of a roll-to-roll system is presented. In all roll-to-roll applications, tension and velocity must be accurately controlled to desired reference trajectories to ensure a quality finished product. Additionally, a registration error model is presented for the control design. Minimization of the registration is the primary objective for flexible electronics, but web tension and velocity cannot be neglected. The model is needed in order to formulate a methodology that can simultaneously control tension, velocity, and registration error in the presence of disturbances.

Micro and nano-scale features are susceptible to damage from friction between the web and the roller. Therefore, tension estimation techniques is highly desired to eliminate load cells from the system. The reduced order observer, extended Kalman filter, and an unknown input observer is presented.

Development of tension and velocity control strategies have historically revolved around decentralized SISO control schemes. In order to achieve higher precision, a centralized MIMO strategy is proposed and compared to decentralized SISO. The advantage of the MIMO controller improved handling of the tension velocity coupling in

roll-to-roll systems. The tension observer is introduced to the control design and evaluated for overall effectiveness.

In simulation, the centralized MIMO control with the unknown input observer demonstrated superior tension and velocity tracking as well as minimal registration error. Development of the proposed MIMO control strategy can enable flexible electronic fabrication using roll-to-roll manufacturing.

Table of Contents

List of Tables

List of Figures

1 INTRODUCTION

1.1 BACKGROUND

Roll-to-Roll (R2R) manufacturing refers to any processing technique applied on a roll of flexible material that is unwound from an unwind roller, undergoes web processing, and rewound onto a rewind roll as a finished product. Some applications of R2R include paper, textiles, coatings, metal foils, coatings, and other thin-films. In recent years, the production of flexible electronics has gained popularity as a low cost high throughput manufacturing process. Examples of flexible electronics produced using R2R include solar panels, thin-film batteries, electric circuits, displays, and sensors [1].

Combining roll-to-roll manufacturing with the flexible electronic industry has enormous potential in making a sustainable, low cost, and mass producible process, leading to further advancement of the industry. The advantage of roll-to-roll lies in the fact that the material is processed continuously during web transfer, rather than conventional manufacturing methods such as batch processing. The global flexible electronics market is expected to grow to $13.23 billion in 2020 [1]. To meet the global market demand, advancements in manufacturing productivity is necessary.

During production, tension and velocity must be closely regulated to prevent stretching or wrinkling of the web. Real time controllers must be designed to meet this demand. An additional requirement for flexible electronics is minimizing the registration error, which is defined as the displacement error between printed components. Furthermore, as the industry moves towards micro and nano-scale applications, there is a need for high performance controllers that can meet these tolerances.

1.2 MOTIVATION

Recently, roll-to-roll manufacturing has been considered for producing micro and nano-scale products in the field of flexible electronics. The advantages of R2R processing compared to traditional methods(deposition, etching, printing) include lower energy costs

and higher throughput per unit area of material [1]. However, precision at the sub micrometer level must be guaranteed to ensure a quality finished product.

The main challenge in controls for R2R machines is maintain proper tension and velocity in the material while minimizing the registration error in the printed components. Proper tension and velocity control is necessary to prevent web breaks, wrinkling, slips, and other material defects in the finished product. Registration error is the displacement error between the printed feature and the desired location. Improper alignment of components can lead to lower quality or a completely dysfunctional finished product, in the case of electronic circuits for example. Therefore, the goal of this research is to design a control strategy for a R2R machine that will meet performance requirements for micro- and nano-manufacturing.

In addition, one of the challenges of roll-to-roll is the high initial capital cost [1]. One method of designing more economic systems is the reduction of sensors in the systems by replacing them with estimators. Therefore, we will also explore methods to estimate the web tension in roll-to-roll systems.

Since we are interested in implementation of real time control in the future, the control framework must also account for uncertainties and disturbances in the system. This must be addressed in the control algorithm and the observer design to ensure proper control effort and estimation of tension.

Due to the developments in micro- and nano-scale manufacturing and desire to produce high quality flexible electronics efficiently and economically, there is a need to develop improved control algorithms for roll-to-roll manufacturing in order to make flexible electronic fabrication feasible.

2 LITERATURE SURVEY

To develop an improved control methodology for roll-to-roll systems, an extensive review of existing modelling, control, and estimation techniques was conducted. While the focus of the research is in minimization of registration error, the controller must also perform well in tension and velocity tracking. Thus, state of the art in tension and velocity modeling and control must be included in the control design. Additionally, the relationship between system states and registration must be understood for the control formulation.

2.1 SYSTEM MODEL

A number of models based on fundamental laws exist which model general web and roller behavior [2–5]. Some assumptions must be made to use this basis model. The web material must be thin compared to the size of the roller to treat the radii of the unwind and rewind roller as time invariant. To relate strain and tension using Hooke's law, the material must be assumed to be elastic. Additionally, these relations only apply when the machine is in operation under tension (in other words, no sagging between rollers). Idle roller dynamics are neglected at steady state operation [5]. No slip is assumed at the point of contact between the web and the roller [4]. This model can be found in many control designs because many roll-to-roll machines operate under these assumptions.

The fundamental model can be expanded by including effects from web processing, roller dynamics, and other physical phenomena. Temperature changes can affect the elastic modulus of the web and need to be included in processes that involve heating or cooling [6–8]. Vedrines and Knittel improved the sliding friction model in [9]. Non-ideal, or eccentric, roller modeling can be found in [10–12]. For 2-D modeling of the web, lateral and longitudinal dynamics can be found in [13,14]. Dynamics of viscoelastic webs was developed in [15]. The effect of backlash in gear driven rollers was modeled in [16]. Wu et al. modeled taper winding to characterize internal stress on a center-wound roll [17].

For the scope of the research, the fundamental model is sufficient for control design. Details of the model and derivation will be presented in Section 3. The effect of fabrication

processes is assumed to be negligible compared to the tension and velocity of the web, especially since we are considering micro and nano scale features on a large continuous web. However, adding complexity to the model can be considered in the future if performance requirements are not met or advances in control technology allow for higher order models to run in real time. Web processing is not considered for the research because the framework that is developed is for general roll-to-roll systems without a specific manufacturing process in mind. However, process modeling should be considered when designing for a real machine.

Overall, the modeling of roll-to-roll systems is well developed. Motivation to update the fundamental models mainly comes from new technological advancements and applications.

2.1.1 Registration Error

Modeling of registration error was conducted to understand the relationship between the error and web dynamics. It is important to minimize registration error in flexible electronics as excessively large error will lead to low quality or even nonfunctioning finished products. Models on registration error can be found in [18–22]. These models describe the relationship between longitudinal registration error and web dynamics. However, the models are limited to only single layer printed applications. Liu et al extended the model to include multilayered printing [23]. Kang et al. modeled the oblique directional registration error in [24].

Much of the literature focuses on longitudinal registration error, or in other words, the direction of the moving web. Lateral error is often neglected since the error is typically much smaller than longitudinal error. For our research, registration error refers to only longitudinal error. The registration model is readily derived from geometric relationships in a roll-to-roll machine and will be described in detail in Section 3.2. The purpose of the model is to understand the relationship between the tension and velocity of the web and the registration error to design a controller. The single layer registration model is used for the work in this thesis.

2.2 CONTROL

Numerous approaches to tension and velocity control have been studied in literature. Decentralized PID controllers have been successfully implemented for a variety of applications [17,25–29]. With accurate models, feedforward control can be used to compensate for known disturbances [18,30].Linear optimal controllers have also been designed based on H_∞ [31–36], H_2 [37], and time optimal [38]. Sliding mode control has been used to improve performance against modeling uncertainty and disturbances [39–42]. Backstepping technique was used to design globally stable controls [43–46]. Active disturbance rejection controller had also been used to estimate and compensate for disturbances to the system [47–49].

Control literature on R2R machines have extensively covered tension and velocity requirements. However, registration error control has become an increasingly important topic in the field of flexible electronics. Choi et al. designed a backstepping registration error control [21]. Liu et al. designed a decoupling control using feedforward and ADRC [47]. Kang et al. used a compensator based on variation in print phase with PID controller [18]. Lee et al. investigated dominating factors in registration error using a PID control scheme [50]. Seshadri and Pagilla developed decentralized memoryless state feedback control [51]. Chen et al. optimized a feedforward PD control using a membrane inspired algorithm [52]. Yang et al. applied sliding mode control to minimize registration error [41]. Kang and Baumann designed a Linear Quadratic Regulator for registration error [20].

Overall, multiple approaches to tension and velocity control had been extensively studied in literature. Linear control strategies have been proven to have acceptable performance in both simulation and experimentally. Likewise, nonlinear controllers have shown excellent results. However, the systems studied in literature do not include high precision machines with high tolerance required for flexible electronics. Furthermore, research has been focused on large scale systems where decentralized controllers are preferred for scalability without increasing controller order. In order to meet performance requirements, we explore the performance improvements a centralized controller would have over decentralized control.

Another comment on the control literature is the lack of focus on registration error minimization. Historically, roll-to-roll manufacturing had been used to create uniform web of materials. Only in recent years has roll-to-roll manufacturing has involved printed features requiring position alignment.

A last point worth mentioning is that the literature focuses on longitudinal web control, in other words, along the direction of movement. In roll-to-roll machines, there is typically a separate lateral guide system to keep the web aligned during transport. Lateral web control can be further explored to explain the dynamics of web slippage and whether control is possible without the use of a guidance system.

2.3 STATE ESTIMATION

Estimation of the web tension is highly valuable in R2R web processing machines. In the absence of estimators, load cells must be installed in systems to provide tension feedback. Use of load cells lead to higher economic cost in the machine design [19]. Furthermore, frictional contact between load cell and web can lead to material degradation or damage [53]. Lack of space can also limit the availability of tension sensors [54]. Examples of estimators that use velocity or motor torque can be found in [54,55]. Gassmann and Knittel applied a Kalman filter using the linearized model as well as the nonlinear Kalman filter on the nonlinear model [56]. Lin et al. developed PI observers that includes the effects of friction and inertia of the rollers[57], and the PI gains were determined through frequency analysis in [58]. Gassmann and Knittel developed an optimized H-∞ PI which has performance improvements over Kalman filtering techniques [59]. Nonlinear observers and sliding mode observers have been developed and compared to linear type observers in [60,61]. The techniques described so far have mainly used web velocity measurements to perform the estimation, but other methods exist. Lee et al. used registration error measurements and the elastic registration error model to inversely estimate the tension [50]. Cheng et al. indirectly estimates tension by first estimating the load torque on the unwind roller [53].

Tension estimators are highly desirable for flexible electronic fabrication. Tension sensors would risk damaging or degrading the electronic features on the web. To develop a complete control system, a highly accurate estimator will need to be developed. Furthermore, the estimation must be accurate even with modeling uncertainties and disturbances.

2.4 OBJECTIVE

The objective of this research is to develop a complete control framework that will meet the needs of flexible electronic fabrication using roll-to-roll technology. In order to meet this objective, an extensive literature survey was conducted to identify existing control technology. The contribution of this thesis is a novel centralized observer-based MIMO control strategy utilizing existing system models and estimation techniques found elsewhere in literature. Three candidate tension observers were selected and a comparative study was conducted to identify the most suitable observer for control design.

3 SYSTEM MODEL

3.1 PHYSICAL SYSTEM

The three main components in a general roll to roll system are the rewind roller, unwind roller, and the web of material. The system can be expanded by the addition of intermediate rollers which help support the web during transport and processing. These rollers may be motor driven or free rollers. Rollers free to rotate are also known as idle rollers. Intermediate rollers are added to systems in order provide structural support to long spans of web during the transport and change the direction of the web. Driven intermediate rollers provide additional control actuation to the system. A schematic of the roll-to-roll system used for control design is shown in Figure 1.

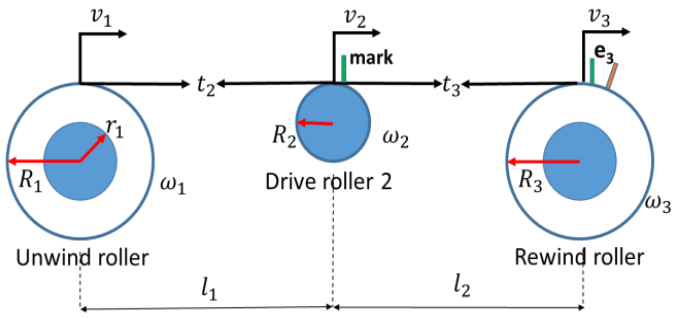

Figure 1. A schematic of a simple R2R system including registration error

Based on the model derivation from Pagilla et al, the dynamic equations for the system shown in Figure 1 is as follows [62]. System dynamics will be discussed in the following while registration error modeling can be found in Section 3.2.

First, the dynamics of the unwind roller is derived as follows. Radius r_1 is the radius of the roller, while R_1 includes the outer roll of material. The inertia, J_1, of the unwind roller can be written as follows[62]:

$$J_1(t) = \frac{\pi}{2} w\rho(R_1^4(t) - r_1^4) \quad (1)$$

Where *w* is the web width, and *p* is the density of the web. The velocity of the unwind roll can be written as follows[62]:

$$\frac{d}{dt}(J_1\omega_1) = \dot{J}_1\omega_1 + \dot{\omega}_1 J_1 = t_1 R_1 - u_1 - b_{f_1}\omega_1 \quad (2)$$

Where u_1 is the motor input, and b_{f_1} is the coefficient of friction between the roller and the web. The motor input is assumed to be a velocity input, while literature typically includes motor armature inertia, gearing ratio, etc.[62]. From Equation 1, the change in roller inertia can be derived as follows[62]:

$$\dot{J}_1 = 2\pi w\rho R_1^3 \dot{R}_1 \quad (3)$$

The velocity of the web, v_1, is related to the angular velocity by $v_1 = R_1\omega_1$. Therefore, the change in angular velocity can be written as follows[62]:

$$\dot{\omega}_1 = \frac{\dot{v}_1}{R_1} - \frac{\dot{R}_1 v_1}{R_1^2} \quad (4)$$

By substituting Equations 3 and 4 into 2, the velocity dynamics can be rewritten and simplified as[62]:

$$\frac{J_1\dot{v}_1}{R_1} = t_2 R_1 - u_1 - \frac{b_{f_1} v_1}{R_1} + \frac{\dot{R}_1 v_1 J_1}{R_1^2} - 2\pi w\rho R_1^2 \dot{R}_1 v_1 \quad (5)$$

The rate of change of the radius R_1 is a function of the velocity and web thickness, t_ω, and can be approximated as the following[62]:

$$\dot{R}_1 \approx -\frac{t_\omega v_1}{2\pi R_1} \quad (6)$$

The relationship is approximated since the radius will only change after a full rotation rather than continuously. However, the web thickness is generally very small so the approximation is valid[62]. By substituting Equation 6 into Equation 5, the velocity dynamics can be simplified to the following[62]:

$$\frac{J_1\dot{v}_1}{R_1} = t_2R_1 - u_1 - \frac{b_{f_1}v_1}{R_1} - \frac{t_\omega}{2\pi R_1}\left(\frac{J_1}{R_1^2} - 2\pi w\rho R_1^2\right)v_1^2 \quad (7)$$

The tension dynamics can be derived using conservation of mass applied around the web span between two rollers. For the tension span downstream of the unwind roller, the tension dynamics is given as follows[62]:

$$l_1\dot{t}_2 = AE(v_2 - v_1) + t_1v_1 - t_2v_2 \quad (8)$$

where A is the cross-sectional area of the web, E is the elastic modulus of the web material, and t_1 is the wound-in tension in the unwind roller.

Similarly, the fundamental principles used to derive dynamic equations for the unwind roller can be applied to the drive roller and the rewind roller. The drive roller is simpler than the other two rollers since there is no center wound roll of material. The velocity dynamics of drive roller 2 is given as follows[62]:

$$\frac{J_2\dot{v}_2}{R_2} = (t_3 - t_2)R_2 + u_2 - \frac{b_{f_2}v_2}{R_2} \quad (9)$$

Finally, the web dynamics for the rewind roller can be given as follows [62]:

$$\frac{J_3\dot{v}_3}{R_3} = t_3R_3 - u_3 - \frac{b_{f_3}v_3}{R_3} - \frac{t_\omega}{2\pi R_3}\left(\frac{J_3}{R_3^2} - 2\pi w\rho R_3^2\right)v_3^2 \quad (10)$$

$$l_2\dot{t}_3 = AE(v_3 - v_2) + t_2v_2 - t_3v_3 \quad (11)$$

3.1.1 Linearization

Equations 7-11 describe a nonlinear set of dynamic equations for the roll-to-roll system. To achieve tension and velocity control objectives, the system is linearized around a tension and velocity reference point, so that a control framework may be

designed. First, the variations in states and inputs from the reference point are defined as follows:

$$\boldsymbol{T_i = t_i - t_{ri}} \tag{12}$$

$$\boldsymbol{V_i = v_i - v_{ri}} \tag{13}$$

$$\boldsymbol{U_i = u_i - u_{ieq}} \tag{14}$$

Where T_i is the tension variation, t_{ri} is the tension reference, V_i is the velocity variation, v_{ri} is the velocity reference, U_i is the input variation, and u_{ieq} is the input required to maintain the desired tension and velocity references. Combining equations 12-14 with 7-11, and canceling out reference terms with the equilibrium input, the system can be rewritten into the following linearized set of equations

For the unwind roller[62]:

$$\boldsymbol{l_1\dot{T}_2 = AE(V_2 - V_1) + t_1V_1 - T_2v_{r_2} - V_2t_{r_2}} \tag{15}$$

$$\boldsymbol{\frac{J_1\dot{V}_1}{R_1} = T_2R_1 - U_1 - \frac{b_{f_1}V_1}{R_1} - \frac{w}{2\pi R_1}\left(\frac{J_1}{R_1^2} - 2\pi b\rho {R_1}^2\right)\left(V_1^2 + 2v_{r_1}V_1\right)} \tag{16}$$

For the drive roller 2[62]:

$$\boldsymbol{\frac{J_2\dot{V}_2}{R_2} = (T_3 - T_2)R_2 + U_2 - \frac{b_{f_2}V_2}{R_2}} \tag{17}$$

For the rewind roller[62]:

$$\boldsymbol{l_2\dot{T}_3 = AE(V_3 - V_2) + t_{r_2}V_2 + T_2v_{r_2} - T_3v_{r_3} - V_3t_{r_3}} \tag{18}$$

$$\boldsymbol{\frac{J_3\dot{V}_3}{R_3} = -T_3R_3 + U_3 - \frac{b_{f_3}V_3}{R_3} + \frac{w}{2\pi R_3}\left(\frac{J_3}{R_3^2} - 2\pi b\rho {R_3}^2\right)\left(V_3^2 + 2v_{r_3}V_3\right)} \tag{19}$$

For the control design, Equations 15 – 19 are arranged into the following state space formulation:

$$\dot{\boldsymbol{x}} = \boldsymbol{\Lambda x} + \boldsymbol{Bu} \quad \textbf{(20)}$$

$$\boldsymbol{y} = \boldsymbol{Cx} + \boldsymbol{Du} \quad (21)$$

Where coefficient matrices are defined as follows [62]:

$$\Lambda = \begin{bmatrix} -\frac{v_{r_2}}{l_1} & \frac{t_1 - AE}{l_1} & \frac{AE - t_{r_2}}{l_1} & 0 & 0 \\ \frac{R_1^2}{J_1} & a_{22} & 0 & 0 & 0 \\ -\frac{R_2^2}{J_2} & 0 & -\frac{b_{f_2}}{J_2} & \frac{R_2^2}{J_2} & 0 \\ \frac{v_{r_2}}{l_2} & 0 & \frac{t_{r_2} - AE}{l_2} & -\frac{v_{r_3}}{l_2} & \frac{AE - t_{r_3}}{l_2} \\ 0 & 0 & 0 & -\frac{R_3^2}{J_3} & a_{55} \end{bmatrix}$$

$$a_{22} = -(\frac{wv_{r_1}}{\pi R_1^2} - \frac{2wb\rho v_{r_1} {R_1}^2}{J_1} + \frac{b_{f_1}}{J_1})$$

$$a_{55} = -(-\frac{wv_{r_3}}{\pi R_3^2} - \frac{2wb\rho v_{r_3} {R_3}^2}{J_3} + \frac{b_{f_3}}{J_3})$$

$$B = \begin{bmatrix} 0 & 0 & 0 \\ -\frac{R_1}{J_1} & 0 & 0 \\ 0 & \frac{R_2}{J_2} & 0 \\ 0 & 0 & 0 \\ 0 & 0 & \frac{R_3}{J_3} \end{bmatrix} \qquad C = \begin{bmatrix} 1 & 0 & 0 & 0 & 0 \\ 0 & 1 & 0 & 0 & 0 \\ 0 & 0 & 1 & 0 & 0 \\ 0 & 0 & 0 & 1 & 0 \\ 0 & 0 & 0 & 0 & 1 \end{bmatrix} \qquad D = 0$$

The state vector, *x*, is defined as $x^T = [T_2, V_1, V_2, T_3, V_3]$, where T_2 and T_3 are linearized t_2 and t_3, and V_1, V_2, and V_3 are linearized v_1, v_2, and v_3. The inputs to the system are the disturbance in motor inputs to the rollers. The control input matrix is defined as $U = [U_1, U_2, U_3]$, where U_1, U_2 and U_3 are motor torque inputs to the unwinding roller, drive roller 2, and rewinding roller, respectively. The system output vector is defined as $y^T = [T_2, V_1, V_2, T_3, V_3]$.

All the parameters for the roll-to-roll system used in the simulation is given in Table 1.

Parameters	Values	Units
Length of span 1 (L_1)	0.3	m
Length of span 2 (L_2)	0.3	m
Reference velocity	0.1	m/s
Reference tension	50	N
Web cross sectional area(A)	25	mm^2
Web's Young's modulus (E)	3000000	Pa
Effective friction constant	0.000685	(N*ms/rad)
Inertia of roller (J_{c0})	7.39E-06	$kg*m^2$
Radius of roller (r_0)	9.925	mm
Initial number of web layers	30	-

Table 1. System Parameters

These parameters are based on an experimental platform from another research group at UT and may be used for experimental validation in the future [63].

3.1.2 Relative Gain Array Analysis

One of the factors in designing an appropriate control strategy for a MIMO system is the coupling between the input and output variables. For a low coupled dynamics system, the system may be decomposed and a decentralized SISO control formulation can perform well. However, for a highly coupled system will require a MIMO controller. For this thesis, relative gain array(RGA) is used to quantify the level of coupling in the roll-to-roll system. The RGA matrix is calculated by the following [64]

$$\boldsymbol{RGA}\ (\boldsymbol{G}) = \boldsymbol{G}\ \boldsymbol{X}\ (\boldsymbol{G^{-1}})^{\boldsymbol{T}} \tag{22}$$

Where *X* denotes element-wise multiplication and *G* is the transfer function of the system. If the RGA matrix is close to diagonal, the closed loop system can be divided into multiple SISO systems [64].

For the roll-to-roll system given in Figure 1, the three inputs are motor torques u_1, u_2, and u_3 and three output velocities are v_1, v_2 and v_3. Several steady-state RGA matrices were calculated with different web material layers on the unwind and rewind rollers.

30 layers on unwind, 0 layer on rewind			
	U_1	U_2	U_3
V_1	40.95	0.00	-39.95
V_2	-39.95	40.95	0.00
V_3	0.00	-39.95	40.95

20 layers on unwind, 10 layer on rewind			
	U_1	U_2	U_3
V_1	45.66	0.00	-44.66
V_2	-44.66	45.66	0.00
V_3	0.00	-44.66	45.66

10 layers on unwind, 20 layers on rewind			
	U_1	U_2	U_3
V_1	45.65	0.00	-44.65
V_2	-44.65	45.65	0.00
V_3	0.00	-44.65	45.65

0 layer on unwind, 30 layers on rewind			
	U_1	U_2	U_3
V_1	40.93	0.00	-39.93
V_2	-39.93	40.93	0.00
V_3	0.00	-39.93	40.93

Table 2. RGA steady state matrices for several web layering conditions

In Table 2, several RGA steady state matrices for four different unwind and rewind layer thickness combinations. In all cases, the RGA matrix is significantly different from identity matrix. This implies that there is high coupling between the input torques and output velocities. This inference provides motivation to design a centralized MIMO controller for the roll-to-roll system. However, a decentralized SISO scheme was

designed and simulated to illustrate the effect of using decentralization on a highly coupled system.

3.2 REGISTRATION ERROR MODEL

Multilayered patterns in flexible electronics must have correct alignment to ensure a high-quality functioning product. The registration error is defined as the positional shift in a point on the web between two references. To minimize the error, an accurate model relating the registration error to the tension and velocity of the web must be developed. The registration error is illustrated in Figure 1. The mark represents a reference point while e_3 represents the error. Mathematically, the registration error model can be defined as follows [21]:

$$\boldsymbol{e_3 = l_2 - \int_{t-L}^{t} r\omega_3 d\tau} \tag{23}$$

Where L is the time lag between adjacent rollers, which is defined as

$$\boldsymbol{L = \frac{l_2}{v_{r2}}} \tag{24}$$

From equation 23 and 24, the registration error is defined as the difference between the length between adjacent rollers, and the integral of the web velocity between the initial time and the time lag. Since the time lag is defined based on the reference velocity in equation 24, the registration error will be zero if the actual web velocity tracked the desired reference velocity. Combining the registration error and the system from equation 20, a controller can be designed to track desired tension, velocity, and registration error simultaneously. Note, that equation 23 assumes that the registration error is only measured between adjacent rollers. The formulation can be extended to more

complex roll-to-roll machines by summing together successive registration errors to calculate the overall error. Equation 23 is sufficient for the control design in this work and will be used in the Section 5.

4 TENSION ESTIMATION

4.1 OVERVIEW

In this section, three different tension estimators will be developed and compared in the simulation. As discussed in Section 1, tension estimators are desirable to eliminate the need for load cells in the roll-to-roll machine. The effectiveness of each estimator will be evaluated by simulation in conjunction with controllers developed in Section 5. Each of the estimation techniques have different advantages such as ease of implementation or accuracy and will be compared and discussed in Section 6.

4.2 REDUCED ORDER LINEAR OBSERVER

Assuming the velocity measurements accurately represent the actual web velocity, a reduced order observer can be developed to estimate only the tension rather than all the states in the case of a full order observer. The reduced order observer framework comes from [65]. The state space form from equation 20 is rewritten to the following[56]:

$$\begin{bmatrix} \dot{x_1} \\ \dot{x_2} \end{bmatrix} = \begin{bmatrix} A_{11} & A_{12} \\ A_{21} & A_{22} \end{bmatrix} \begin{bmatrix} x_1 \\ x_2 \end{bmatrix} + \begin{bmatrix} B_1 \\ B_2 \end{bmatrix} u \tag{25}$$

where

$$A_{11} = \begin{bmatrix} a_{22} & 0 & 0 \\ 0 & -\frac{b_{f_2}}{J_2} & 0 \\ 0 & 0 & a_{55} \end{bmatrix} \qquad A_{12} = \begin{bmatrix} \frac{R_1^2}{J_1} & 0 \\ -\frac{R_2^2}{J_2} & \frac{R_2^2}{J_2} \\ 0 & -\frac{R_3^2}{J_3} \end{bmatrix}$$

$$A_{21} = \begin{bmatrix} \frac{t_1 - AE}{l_1} & \frac{AE - t_{r_2}}{l_1} & 0 \\ 0 & \frac{t_{r_2} - AE}{l_2} & \frac{AE - t_{r_3}}{l_2} \end{bmatrix} \qquad A_{22} = \begin{bmatrix} -\frac{v_{r_2}}{l_1} & 0 \\ \frac{v_{r_2}}{l_2} & -\frac{v_{r_3}}{l_2} \end{bmatrix}$$

$$\boldsymbol{B_1} = \begin{bmatrix} -\dfrac{\boldsymbol{R_1}}{\boldsymbol{J_1}} \\ \dfrac{\boldsymbol{R_2}}{\boldsymbol{J_2}} \\ \dfrac{\boldsymbol{R_3}}{\boldsymbol{J_3}} \end{bmatrix} \qquad \boldsymbol{B_2} = \begin{bmatrix} \boldsymbol{0} \\ \boldsymbol{0} \end{bmatrix}$$

where $x_1 = [V_1,\ V_2,\ V_3]$ and $x_2 = [T_2,\ T_3]$. A_{11}, A_{12}, A_{21}, and A_{22} are rearrangements of the Λ matrix and B_1 and B_2 are from the *B* matrix in equation 20. Hence, x_1 represents the measured velocity states, while x_2 represents the tension states to be estimated. The reduced order observer designed to estimate x_2 is given as follows [66]:

$$\dot{\boldsymbol{z}} = \boldsymbol{Pz} + \boldsymbol{Mu} + \boldsymbol{Ny} \tag{26}$$

$$\dot{\hat{\boldsymbol{x}}}_{\boldsymbol{2}} = \boldsymbol{z} + \boldsymbol{Ly} \tag{27}$$

where

$$P = A_{22} - LA_{12}$$

$$M = B_2 - LB_1$$

$$N = PL + A_{21} - LA_{11}$$

L is the observer gain, *y* is the velocity measurement error, and $\hat{x}_2$ is the tension estimate. The advantage of the reduced order observer is that the order of the observed system is reduced by directly using output measurements rather than through calculation. However, the technique is based on the linearized system from equation 20 and may not perform well on the nonlinear plant. This leads into the extended Kalman filter which can handle not only the nonlinearity, but also noise in the measurements.

4.3 EXTENDED KALMAN FILTER

The R2R system depicted in Figure 1 is a nonlinear, highly coupled system. The above developed reduced order linear observer may have inferior performance when the system is far from the linearization point. Therefore, an extended Kalman filtering

approach may provide better estimate. The following extended Kalman filter comes from [56]. The tension estimate is updated through prediction by using the nonlinear model of the R2R system and the velocity measurement error. The process and measurement noise were assumed to be zero mean Gaussian white noise.

The extended Kalman filter is described as follows. Define the nonlinear state equations in the following form

$$\dot{\boldsymbol{x}} = \boldsymbol{f}(\boldsymbol{x}, \boldsymbol{u}) + \boldsymbol{w} \tag{28}$$

$$\boldsymbol{y} = \boldsymbol{h}(\boldsymbol{x}) + \boldsymbol{v} \tag{29}$$

Where $\boldsymbol{f}(\boldsymbol{x}, \boldsymbol{u})$ is the nonlinear system, *w* is the process noise, *h(x)* is the output and *v* is the measurement noise. Next the prediction-update equations are as follows [56]:

$$\dot{\hat{\boldsymbol{x}}} = \boldsymbol{f}(\hat{\boldsymbol{x}}, \boldsymbol{u}) + \boldsymbol{K}(\boldsymbol{t})(\, \boldsymbol{y} - \boldsymbol{h}(\hat{\boldsymbol{x}})\,) \tag{30}$$

$$\dot{\boldsymbol{P}} = \boldsymbol{F}(\boldsymbol{t})\boldsymbol{P}(\boldsymbol{t}) + \boldsymbol{P}(\boldsymbol{t})\boldsymbol{F}(\boldsymbol{t})^{\boldsymbol{T}} - \boldsymbol{K}(\boldsymbol{t})\boldsymbol{H}(\boldsymbol{t})\boldsymbol{P}(\boldsymbol{t}) + \boldsymbol{Q}(\boldsymbol{t}) \tag{31}$$

$$\boldsymbol{K}(\boldsymbol{t}) = \boldsymbol{P}(\boldsymbol{t})\boldsymbol{H}(\boldsymbol{t})^{\boldsymbol{T}}\boldsymbol{R}(\boldsymbol{t})^{-\boldsymbol{1}} \tag{32}$$

$$\boldsymbol{F}(\boldsymbol{t}) = \frac{\boldsymbol{df}}{\boldsymbol{dx}} \tag{33}$$

$$\boldsymbol{H}(\boldsymbol{t}) = \frac{\boldsymbol{dh}}{\boldsymbol{dx}} \tag{34}$$

Where $\hat{\boldsymbol{x}}$ is the state estimate, *P(t)* is the covariance, *Q(t)* is the process noise, *R(t)* is the measurement noise, and *K(t)* is the Kalman gain. For the continuous time formulation in equations 30-34, the state estimate, covariance, and Kalman gain equations must be solved simultaneously because the prediction and update steps are coupled.

4.4 UNKNOWN INPUT OBSERVER

In a real manufacturing process, the R2R plant is subject to unknown input disturbances and plant uncertainties. Both the reduced order linear observer and the extended Kalman filter estimate states by using the output measurement error. A unknown input observer (UIO) can be designed to provide better estimates if the disturbance can be modeled as an input, even if disturbance is unknown. The unknown input observer formulation comes from [67] and will be presented in this section. A system with disturbance can be modeled in state space form as follows [67]:

$$\dot{\boldsymbol{x}} = \boldsymbol{Ax} + \boldsymbol{Bu} + \boldsymbol{Ed} \tag{35}$$

$$\boldsymbol{y} = \boldsymbol{Cx} + \boldsymbol{Du} \tag{36}$$

where *E* is the unknown input distribution and *d* is the unknown disturbance. The unknown input distribution models the disturbance as an additive term to the state model. The necessary and sufficient conditions for designing the UIO are as follows [67]:

1) $Rank(CE) = Rank(E)$
2) $(A_1, C)\ is\ observable, where\ A_1 = A - E[(CE)^T CE]^{-1}(CE)^T CA$

In a roll-to-roll machine, we assume most disturbances will occur at the driven rollers especially compared to web transport sections. Furthermore, disturbances on the web can be lumped together with the input disturbances due to the coupling between the web dynamics and input. Therefore, *E* can be defined as the input matrix B to check necessary and sufficient conditions. The conditions are met in our simulation and the simulation results will be presented in Section 6.

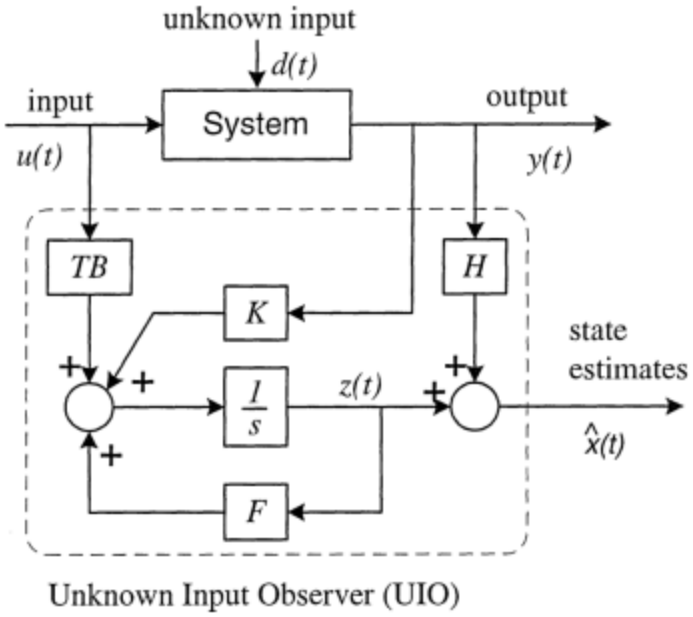

Figure 2. Structure of Unknown Input Observer[67]

In order to implement the unknown input observer in Figure 2, the blocks *F, T, K, H* must be calculated. From [67], the following observer matrices are defined[67]:

$$\boldsymbol{H} = \boldsymbol{E}[(\boldsymbol{CE})^{\boldsymbol{T}}\boldsymbol{CE}]^{-\boldsymbol{1}}(\boldsymbol{CE})^{\boldsymbol{T}} \tag{37}$$

$$\boldsymbol{T} = \boldsymbol{I} - \boldsymbol{HC} \tag{38}$$

$$\boldsymbol{A_1} = \boldsymbol{TA} \tag{39}$$

Before proceeding with the observer design, the pair (C, $\boldsymbol{A_1}$) must be detectable. If the pair is observable, then the unknown input observer exists and the observer pole K_1 can be calculated using pole placement. If the pair is not observable, an observable canonical decomposition can be constructed, and the instructions can be found in [67]. Once a desirable observer pole has been selected, the following matrices can be calculated and the observer scheme in figure can be used:

$$\boldsymbol{F = A_1 - K_1 C} \tag{40}$$

$$\boldsymbol{K = K_1 + FH} \tag{41}$$

Note, in figure , the system refers to the linearized state space model. Therefore, the unknown input observer is a linear type. Furthermore, the formulation presented in this section is full order and estimates all the states including the measured velocity output. The additional advantage of this methodology is that measurement errors can be detected and compensated for as it is treated as input disturbance.

5 CONTROL METHODOLOGY

5.1 PROBLEM FORMULATION

The control objective for this study is defined as the following: Track tension and velocity to desired references and minimize the registration error. In order to achieve this objective, a linear quadratic regulator, or LQR, framework is proposed. LQR has been widely used in optimal control theory to track a state trajectory while minimizing state error and control input according to a cost function. For this research, we will examine two variations of LQR: decentralized and centralized. Decentralized controllers have been widely implemented in roll-to-roll systems, and a decentralized LQR scheme was formulated to represent the state of the art. A novel centralized LQR is proposed to demonstrate significant tracking performance compared to the decentralized scheme.

Furthermore, the effectiveness of each tension estimator from Section 4 will be studied in conjunction with the control design. The objective is to determine if the controller can perform well without relying on tension sensors.

5.2 LINEAR QUADRATIC REGULATOR

In optimal control theory, the objective is to operate a dynamic system at minimum cost. For the linear quadratic regulator, the cost, J, is defined as follows:

$$\boldsymbol{J} = \int \boldsymbol{x^T Q x} + \boldsymbol{u^T R u} \tag{42}$$

Where x is the state error, u is the control input, Q is the state weighting function, and R is the input weighting function. For the roll-to-roll system, the state and input vector differ between the decentralized and centralized controller. For the decentralized control, the states and input refer only to the localized variables pertaining to the subsystem. In the centralized controller, the cost function contains the full state and input vectors.

For the simulation in MATLAB, the built in LQR function was used to determine feedback gains. The weights, Q and R, were taken to be identity matrices. These weights should be tuned for control objectives desired of the real system. For simulation purposes, these weights need only to be held constant between trials to compare the effectiveness of different control strategies.

5.3 Feedforward Control

One of the most fundamental control methods is the feedforward control. In this design, a control input is calculated offline based on the model inverse and desired reference trajectory. The formulation of a feedforward control gain *N is* as follows [68]:

$$\boldsymbol{N = -(C_z(A)^{-1}B)^{-1}} \tag{43}$$

Where

$$C_z = \begin{bmatrix} 1 & 0 & 0 & 0 & 0 \\ 0 & 0 & 0 & 1 & 0 \\ 0 & 0 & 0 & 0 & 1 \end{bmatrix}$$

The feedforward compensation is calculated as follows:

$$\boldsymbol{u = Nr} \tag{44}$$

Where *r* is the desired reference, and *u* is the control input.

5.4 Decentralized SISO Control

For large scale roll to roll systems, decentralized controllers have been used extensively. The benefit of a decentralized scheme is the scalability into large systems without increasing the controller order. The disadvantage of decentralized control is the lack of compensation for coupling effects between the subsystem. Nevertheless, decentralized control has been used successfully in a wide variety of applications. In this work, a decentralized LQR control is designed to represent the industry standard.

To design the decentralized control, the original system is first subdivided into subsystems. From Figure 3, the original roll-to-roll system is divided into 3 subsystems, based on the tension and velocity pairs on each driven roller.

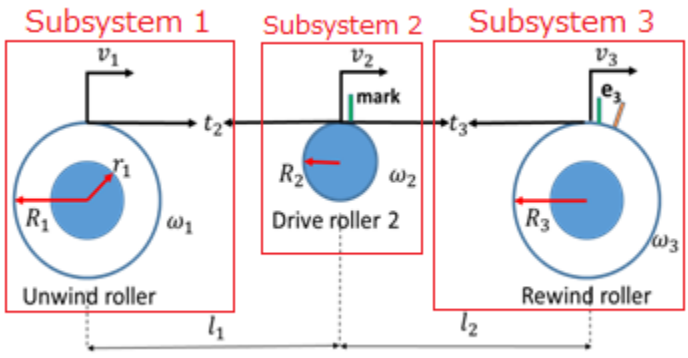

Figure 3. Roll-to-roll system divided into subsystems

The decomposition is based on the physical configuration of the system. Intuitively, a decentralized control system would have a controller for each driven roller with local state information. Using equation 20, the decentralized system can be represented as follows:

$$\dot{\boldsymbol{x}}_{\boldsymbol{sub,1}} = \begin{bmatrix} -\frac{v_{r_2}}{l_1} & \frac{t_1 - AE}{l_1} \\ \frac{R_1^2}{J_1} & a_{22} \end{bmatrix} \boldsymbol{x}_{\boldsymbol{sub,1}} + \begin{bmatrix} 0 \\ -\frac{R_1}{J_1} \end{bmatrix} \boldsymbol{u_1} \tag{45}$$

$$\dot{\boldsymbol{x}}_{\boldsymbol{sub,2}} = \left[-\frac{b_{f_2}}{J_2}\right] \boldsymbol{x}_{\boldsymbol{sub,2}} + \left[\frac{R_2}{J_2}\right] \boldsymbol{u_2} \tag{46}$$

$$\dot{\boldsymbol{x}}_{\boldsymbol{sub,3}} = \begin{bmatrix} -\frac{\boldsymbol{v}_{r_3}}{\boldsymbol{l}_2} & \frac{\boldsymbol{AE} - \boldsymbol{t}_{r_3}}{\boldsymbol{l}_2} \\ -\frac{\boldsymbol{R}_3^2}{\boldsymbol{J}_3} & \boldsymbol{a}_{55} \end{bmatrix} \boldsymbol{x}_{\boldsymbol{sub,3}} + \begin{bmatrix} \boldsymbol{0} \\ -\frac{\boldsymbol{R}_1}{\boldsymbol{J}_1} \end{bmatrix} \boldsymbol{u}_3 \tag{47}$$

Where $x_{sub,1}^T = [T_2, V_1]$, $x_{sub,2}^T = [V_2]$, and $x_{sub,3}^T = [T_3, V_3]$. For each of the three subsystems, a standard LQR methodology was used to design a tracking controller for tracking only the localized tension and velocity variables. Coupling effects from the other subsystems were treated as disturbances to the subsystem. The feedback gains can be calculated as follows using the LQR methodology:

$$\boldsymbol{F}_{\boldsymbol{sub,1}} = [\ \boldsymbol{0.9821} \quad \boldsymbol{-1.0217}] \tag{48}$$

$$\boldsymbol{F}_{\boldsymbol{sub,2}} = \boldsymbol{0.9334} \tag{49}$$

$$\boldsymbol{F}_{\boldsymbol{sub,3}} = [\ \boldsymbol{0.9821} \quad \boldsymbol{1.0218}\ ] \tag{50}$$

Where $\boldsymbol{F}_{\boldsymbol{sub,i}}$ is the feedback gain for subsystem *i*. Next, the control input can be calculated as follows:

$$\boldsymbol{u}_1 = -\boldsymbol{F}_{\boldsymbol{sub,1}}\, \boldsymbol{x}_{\boldsymbol{sub,1}} \tag{51}$$

$$\boldsymbol{u}_2 = -\boldsymbol{F}_{\boldsymbol{sub,2}} \boldsymbol{x}_{\boldsymbol{sub,2}} \tag{52}$$

$$\boldsymbol{u}_3 = -\boldsymbol{F}_{\boldsymbol{sub,3}} \boldsymbol{x}_{\boldsymbol{sub,3}} \tag{53}$$

5.5 CENTRALIZED MIMO CONTROL

In the centralized MIMO control framework, a feedback gain is calculated using the linear quadratic regulation design. The advantage is that coupled dynamics between states are all inclusive in the LQR optimization compared to the decentralized scheme. Furthermore, the motivation to use a MIMO controller is corroborated by the RGA analysis in Section 3.1.2. Instead of using the decomposed subsystems in equations 45-47, the

original linearized dynamic model in equation 20 will be used for control design. Using the LQR function in MATLAB and the system parameters from Table 1, the feedback gain F is as follows:

$$\boldsymbol{F} = \begin{bmatrix} \mathbf{2.4711} & \mathbf{-3.1699} & \mathbf{0.0348} & \mathbf{0.6720} & \mathbf{0.0158} \\ \mathbf{1.8140} & \mathbf{-0.0417} & \mathbf{3.1640} & \mathbf{-1.8122} & \mathbf{-0.0417} \\ \mathbf{0.6722} & \mathbf{-0.0158} & \mathbf{-0.0348} & \mathbf{2.4691} & \mathbf{3.1698} \end{bmatrix} \tag{54}$$

In the closed loop feedback scheme, the control input is calculated as follows:

$$\begin{bmatrix} \boldsymbol{u_1} \\ \boldsymbol{u_2} \\ \boldsymbol{u_3} \end{bmatrix} = -\boldsymbol{F} \begin{bmatrix} \boldsymbol{t_2} \\ \boldsymbol{v_1} \\ \boldsymbol{v_2} \\ \boldsymbol{t_3} \\ \boldsymbol{v_3} \end{bmatrix} \tag{55}$$

5.6 OBSERVER BASED CONTROL DESIGN

Both the decentralized SISO controller in Section 5.4 and the centralized MIMO controller in Section 5.5 rely on feedback of the state vector, $x^T = [t_2, v_1, v_2, t_3, v_3]$. However, one of the control design goals is to eliminate the need for tension feedback from sensors in the roll-to-roll system. A tension observer can be implemented to estimate the tension for the feedback loop. The three tension observers proposed in Section 4 will be used for this purpose. For the centralized MIMO controller, the feedback gain *F* is the same as in equation 54. The difference is that the control input will now use estimated tension states as follows:

$$\begin{bmatrix} \boldsymbol{u_1} \\ \boldsymbol{u_2} \\ \boldsymbol{u_3} \end{bmatrix} = -\boldsymbol{F} \begin{bmatrix} \boldsymbol{\hat{t}_2} \\ \boldsymbol{v_1} \\ \boldsymbol{v_2} \\ \boldsymbol{\hat{t}_3} \\ \boldsymbol{v_3} \end{bmatrix} \tag{56}$$

Where $\hat{t}_2$, and $\hat{t}_3$ are tension 2 and tension 3 estimates, respectively. The method of calculating these estimates vary depending on the selection of observer, however the feedback control will remain the same as in equation 56.

6 SIMULATION AND RESULTS

This section presents the MATLAB/Simulink simulation results from the proposed control design. The goal is to highlight the benefits and drawbacks of each approach. For all simulation cases, the system parameters are the same as in Table 1. Input disturbances ranging from 1% to 15% of equilibrium torques is introduced to the system in order to analyze the control performance under disturbance conditions. Disturbances can originate elsewhere, but for the purpose of simulation, all disturbances are considered to be input disturbance. Since, the disturbance is unknown regardless of the source, we consider the input disturbance as a lump sum of all disturbances that can occur in the roll-to-roll system. Furthermore, various step sized disturbances are simulated to demonstrate both steady state and transient performance of the respective controllers. The motivation in having a variable step profile is to simulate periodic disturbance that occurs in roll-to-roll systems due to eccentricity in the roller; the disturbance is introduced to the system every revolution.

Based on the registration error model in Section 3, the output variables of interest are $T_2, T_3,$ and V_3 since they directly impact the registration error. These state errors will be presented along with the registration error in all the subsequent simulations. For all cases, the tension reference is 50 N and the velocity reference is 0.1 m/s. The total simulation time is set to 35 seconds to illustrate both transient and steady state behavior. These simulation parameters for all test cases are summarized below in Table 3.

Parameters	Values	Units
Reference velocity	0.1	m/s
Reference tension	50	N
Simulation Time	35	s

Table 3. Simulation Parameters

One of the motivation for this research is to demonstrate the capabilities of the control scheme and apply to a real-world machine for experimental validation. Therefore, the simulations were conducted using the nonlinear plant model before linearization. In theory, the control will demonstrate acceptable performance when the system state is near the linearization point, in this case the tension and velocity reference. To prove the effectiveness of the controller, the initial condition is set to zero, in other words, far from the reference, to determine if the control performance is acceptable.

6.1 FEEDFORWARD CONTROL

An open loop analysis was conducted to examine the input-output response of the system without any controllers. The result of the simulation is shown in the following.

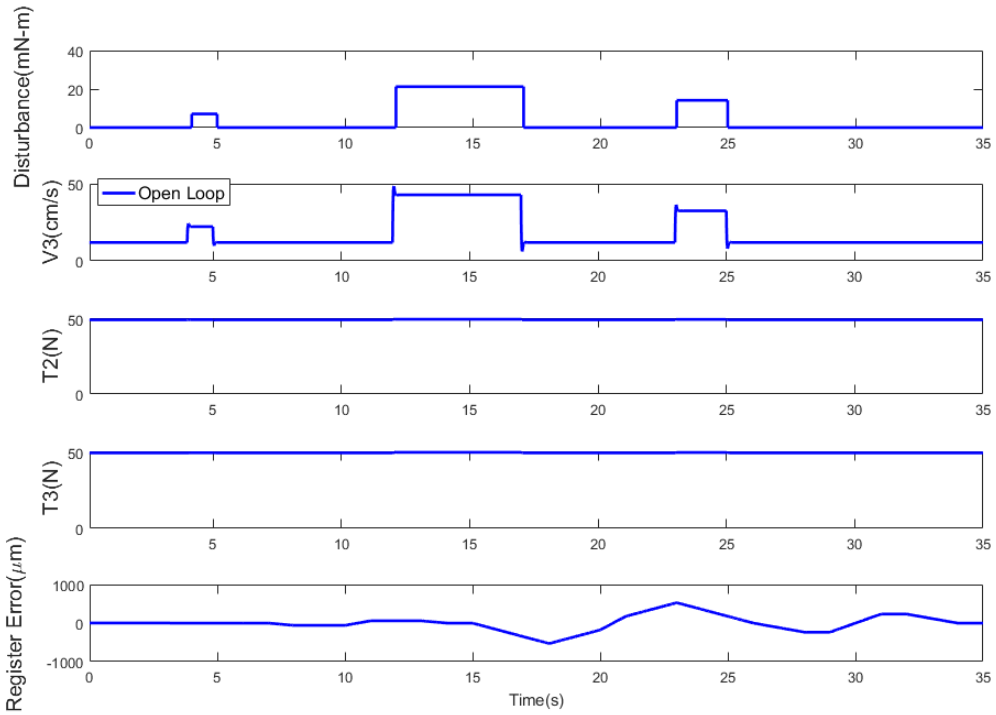

Figure 4. Open Loop Response

Figure 4 shows the state error and registration error for the roll-to-roll system subject to a 15% equilibrium torque disturbance. The top graph was included to show the input disturbance in order to show the effect on the state and registration error. Note that the states , T_2, T_3, V_3, are state errors, not the actual states. Therefore, the ideal tracking scenario is for these state errors to track zero. The last graph in Figure 4 shows the registration error.

In the open loop response, the system is at rest with zero velocity and zero tension until an input disturbance occurs. Note that the tension errors T_2, T_3 are at 50N during steady state since that is the desired reference. The velocity error is 10 cm/s at steady state, which is equivalent to the velocity reference of 0.1 m/s. The results are presented as error rather than actual states to remain consistent with the analysis for the other simulations; The key result to examine in all the results is whether the error tracks zero. At each step disturbance, the system accelerates and moves the web while introducing a small tension to both T_2, T_3. This illustrates the coupling effect between tension and velocity. Note that the peak registration error under these simulation conditions is 528.9 μm.

Next, a feedforward controller was designed to force the system to the desired tension and velocity as formulated in Section 5.3. Without disturbances to the system, including modeling uncertainty, the feedforward controller will be sufficient in tracking state errors. The results of the feedforward controller is compared to the open loop response in the following.

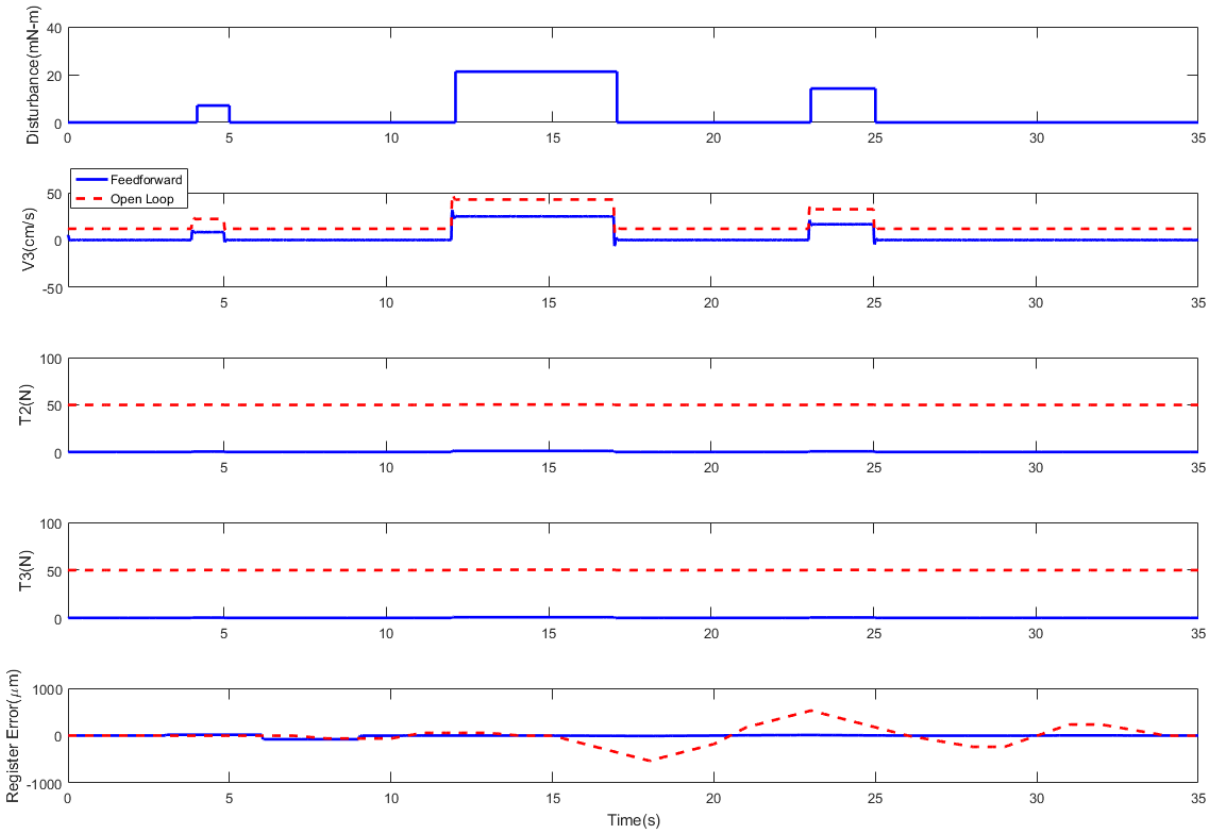

Figure 5. Performance of feedforward control

For the feedforward controller with no tension or velocity feedback control gains, the results demonstrate reasonable performance during steady state with no input disturbances. Compared to the open loop response, the feedforward show zero state error during steady state operation. However, significant errors occur when the input disturbance is introduced. For the velocity, the peak error is 30.95 cm/s, around three times the desired velocity. Both peak tension errors T_2, T_3 are at 0.42 N. The peak registration error is 3.566 μm, a significant improvement from the open loop response.

The errors introduced to the system due the input disturbance demonstrates the lack of robustness from open loop control. Furthermore, perfect tracking under steady state is shown in Figure 5 only under the assumption that the model is perfect; the performance is

expected to deteriorate in experimentation. For these reasons, there is motivation to develop a state feedback control framework even as this controller provides a better baseline for comparison than the open loop simulations.

6.2 FULL STATE FEEDBACK LQR

In this first simulation, control schemes for both decentralized SISO and centralized MIMO control are developed. In this case, tension and velocity states are assumed to be known and used as feedback for the LQR control. In practice, these values are determined from tension sensors and encoders on the driven rollers, which will have uncertainty in the measurement. However, in the current study, the full state feedback controllers were developed to demonstrate the effectiveness of the control law rather than to develop a real controller. The scope of the research is to compare the performance of decentralized and centralized control under the same conditions. Therefore, the tension and velocity measurements are assumed to be exact. First, a decentralized SISO control was developed and compared to the feedforward control performance.

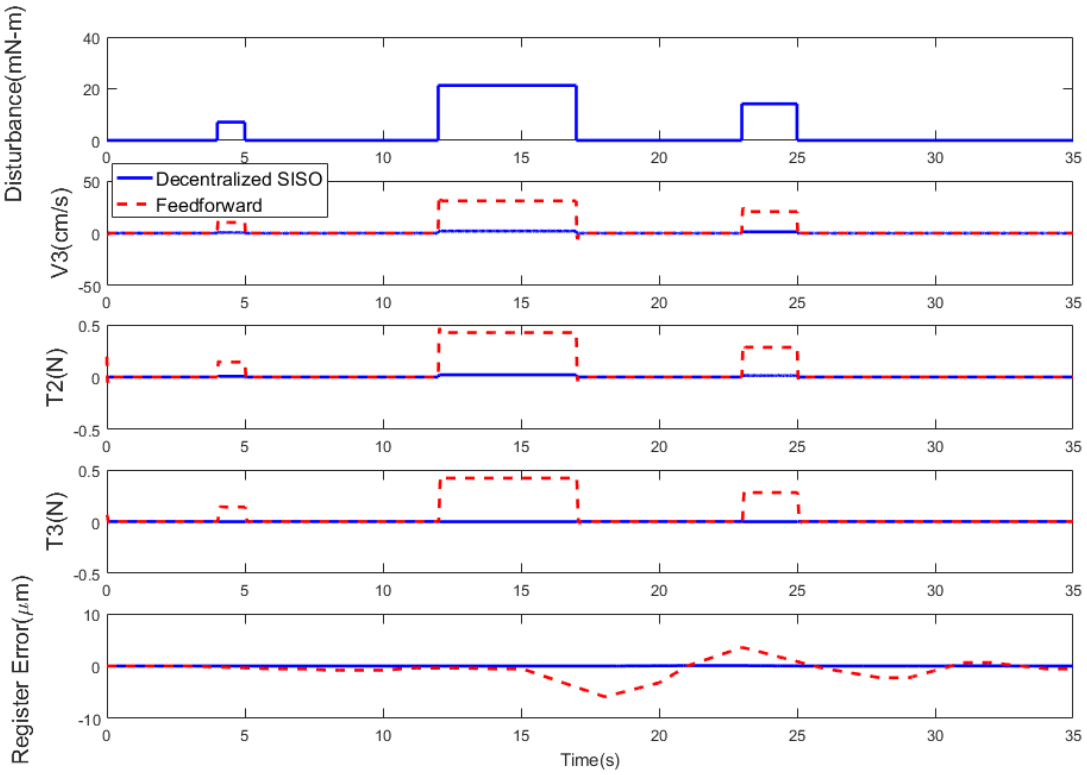

Figure 6. Performance of decentralized SISO vs. feedforward

In Figure 6, the decentralized SISO control drastically reduced the state and registration error. In both cases, the steady state error is zero; the key improvement is the disturbance compensation. By using the decentralized controller developed in Section 5.4, a corrective feedback control action was achieved. Furthermore, the control strategy utilized local state feedback information without regard to the coupling in the overall system. This comparison demonstrates the importance of state feedback in compensating for disturbances and uncertainties in the system.

However, the decentralized SISO controller does not achieve the best performance. In this scheme, each SISO controller treated coupling from adjacent subsystem as disturbances. From Section 3.1.2, the RGA analysis shows strong coupling in the system, more than can be compensated for with decentralized control. Therefore,

we aim to develop a centralized MIMO controller for the roll-to-roll system in order to achieve high precision capability. This controller was developed and compared with the decentralized SISO in the following.

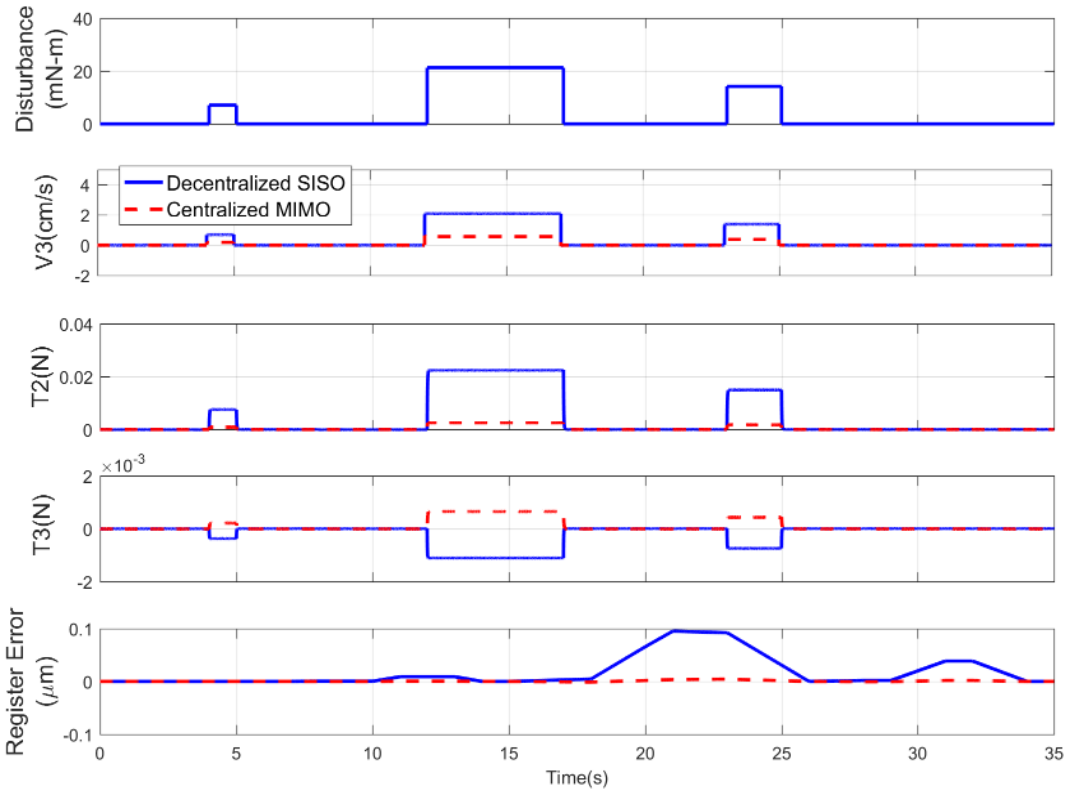

Figure 7. Performance of decentralized SISO vs centralized MIMO with full state feedback

Across all torque disturbance cases, the centralized MIMO controller demonstrated over 10 times smaller registration error. Additionally, the performance in state errors showed significant improvement. For tension error T_3, the errors have opposite signs for the two different controllers. For the decentralized SISO control, the negative tension error signifies undershooting the desired tension reference, while the centralized MIMO controlled showed overshooting. In a web handling system, both

scenarios are equally undesirable. By examining the magnitude of the error, the centralized MIMO outperforms the decentralized SISO control.

The simulation showed that the centralized control has a significant control performance advantage over the decentralized. The disadvantage of computational costs still exists for centralized control for higher order systems and will need to be addressed in the future. However, the results demonstrate that a centralized scheme is needed to meet the high precision requirements in flexible electronic fabrication; the decentralized SISO control underperforms since it treats the coupling effects between tension and velocity as disturbance.

Next, the centralized MIMO control is redesigned to include a tension observer rather than full state feedback. The decentralized SISO with observer is not presented since the full state feedback formulation did not meet performance requirements.

6.3 OBSERVER BASED CONTROL DESIGN

6.3.1 Reduced order

In this simulation, the tension is estimated using the reduced order linear observer. Velocity is assumed to be measured with encoders with no uncertainty and used to predict a tension estimate based on the plant model. Note, the model is from equation 20 which is the linearized realization of the nonlinear plant model. Furthermore, the reduced order observer has dependency on the control input, but unknown to the observer model is the input disturbance. Due to the nonlinearity and disturbances, the observer is expected to have poor performance. Nevertheless, this result is important for future discussion since the reduced order observer is taken as the baseline for comparison. Additionally, the observer has the advantage of ease of implementation, if performance is acceptable.

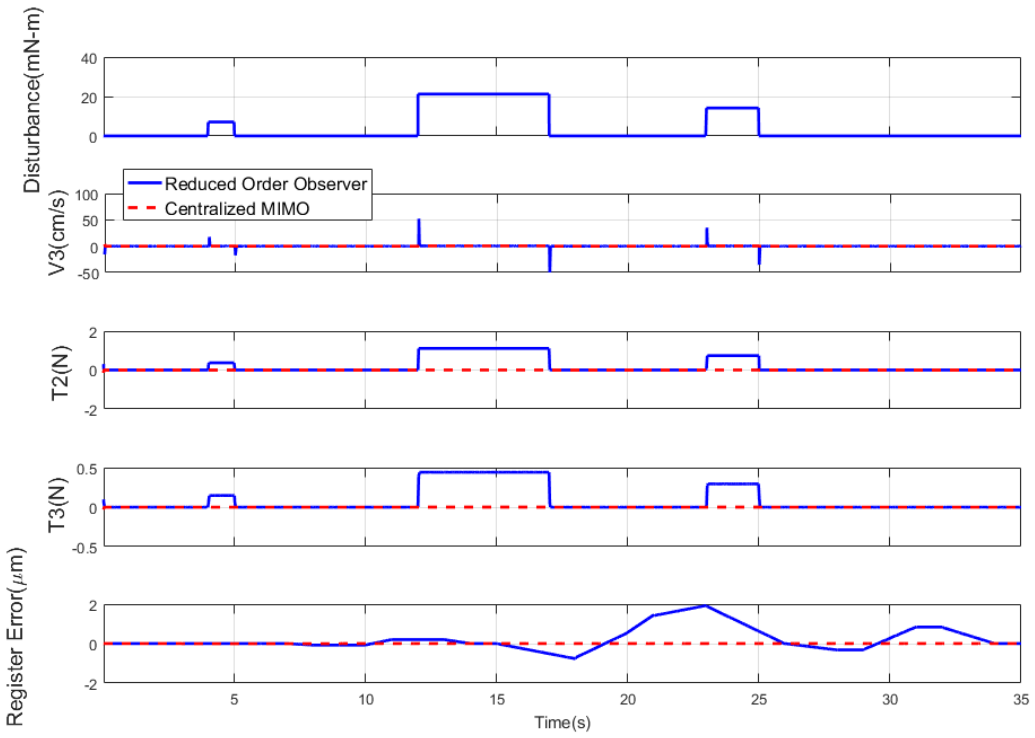

Figure 8. Comparison of centralized MIMO control with reduced order observer and full state feedback

From Figure 8, the centralized MIMO control with the reduced order observer is compared to the full state feedback test case from Section 6.2. The results show a significantly worse performance using the observer, over 1 μm peak registration error. In fact, the result is worse than the decentralized SISO control with full state feedback. The reason for the significant difference in results is mainly due to the presence of the unknown input disturbance. The state errors reach a steady state for the duration of the disturbance. This signifies that the observer did not converge on the true state values in the presence of disturbances.

While the reduced order observer framework is unsuitable for flexible electronic fabrication, the 1 μm registration error would be acceptable for a wide variety of other

roll-to-roll applications that does not require high precision. With an advantage in ease of design and implementation, the reduced order observer can be an efficient method for tension estimation.

6.3.2 Extended Kalman Filter

The extended Kalman filter was designed to address the nonlinear plant. The idea is to improve on the reduced order observer results by creating a framework that can handle a nonlinear model. Furthermore, the formulation includes process and measurement noise, which addresses both any modeling uncertainty and the input disturbance. The noise is assumed to be zero mean Gaussian white noise.

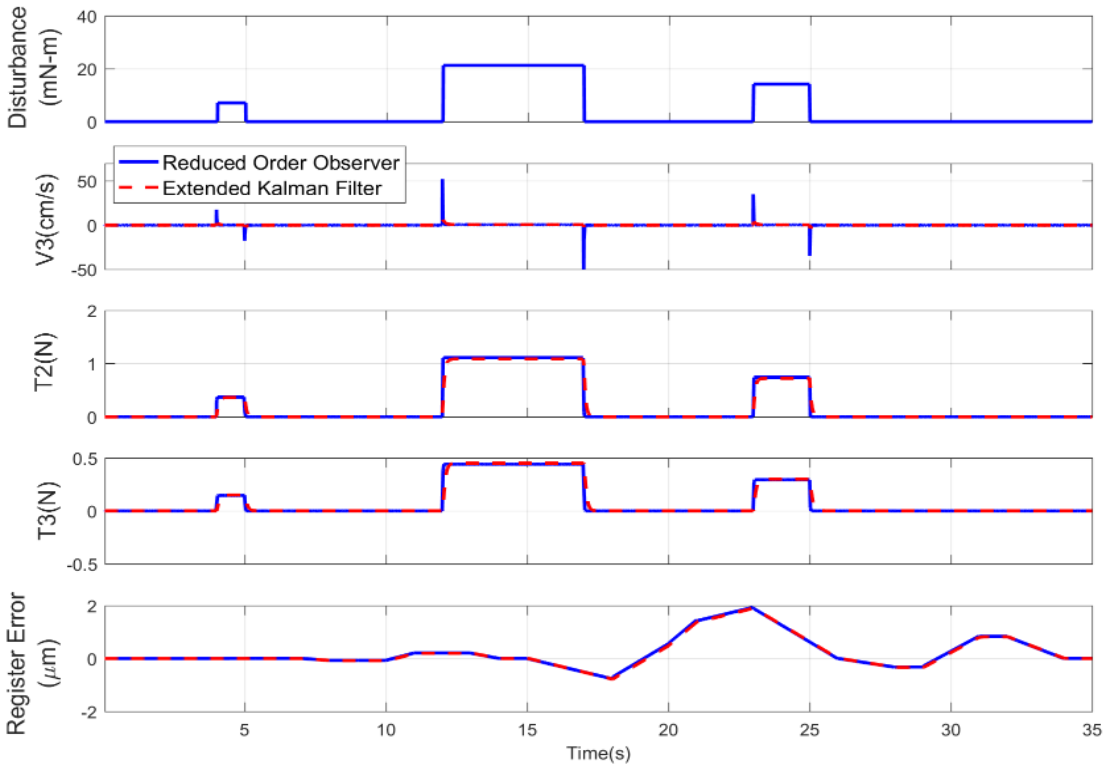

Figure 9. Comparison of the centralized MIMO controller with a reduced order observer and an extended Kalman filter

In Figure 9, the extended Kalman filter performed slightly better than the reduced order observer, but still severely underperforms against the full state feedback controller. For a 15% torque disturbance, the extended Kalman filter results in a peak registration error of 1.8951 μm compared to 1.9305 μm for the reduced order. While the controller with the extended Kalman filter is unsuitable for flexible electronic fabrication, some insights can still be gained. The small difference in results can mostly be attributed to the nonlinearity. If the linear plant was significantly different from the nonlinear plant, the results in Figure 9 would have been much different. Another explanation is modeling the process noise allowed for some of the input disturbance to be compensated. If that is the case, without the noise term in the filter, the results would have been equivalent and corroborate the claim that the linearized plant accurately represented the nonlinear system. On the topic of input disturbance, modeling the noise as Gaussian white noise was insufficient. In the standard extended Kalman formulation, the noise refers to small disturbances, while in our simulation, the input disturbance is significantly higher in magnitudes. Furthermore, the periodic disturbance does not match a white noise model well. For both these reasons, the extended Kalman filter falls short because of inadequate disturbance modeling and compensation.

6.3.3 Unknown Input Disturbance

The third tension observer developed is the unknown input disturbance observer. In this framework, the state space equation is modified to include a disturbance term. The assumption is that the disturbance to the system is linear and superposition principle applies. Furthermore, the control designer must select an appropriate input distribution. In other words, the source of the disturbance must be accurately modeled even if the magnitude of the disturbance is unknown. Knowledge of the input distribution is required in order to verify that necessary conditions are met from Section 4.4. These restrictions limit the type of systems where an unknown input observer may be used, but in applicable problems, the results are quite remarkable.

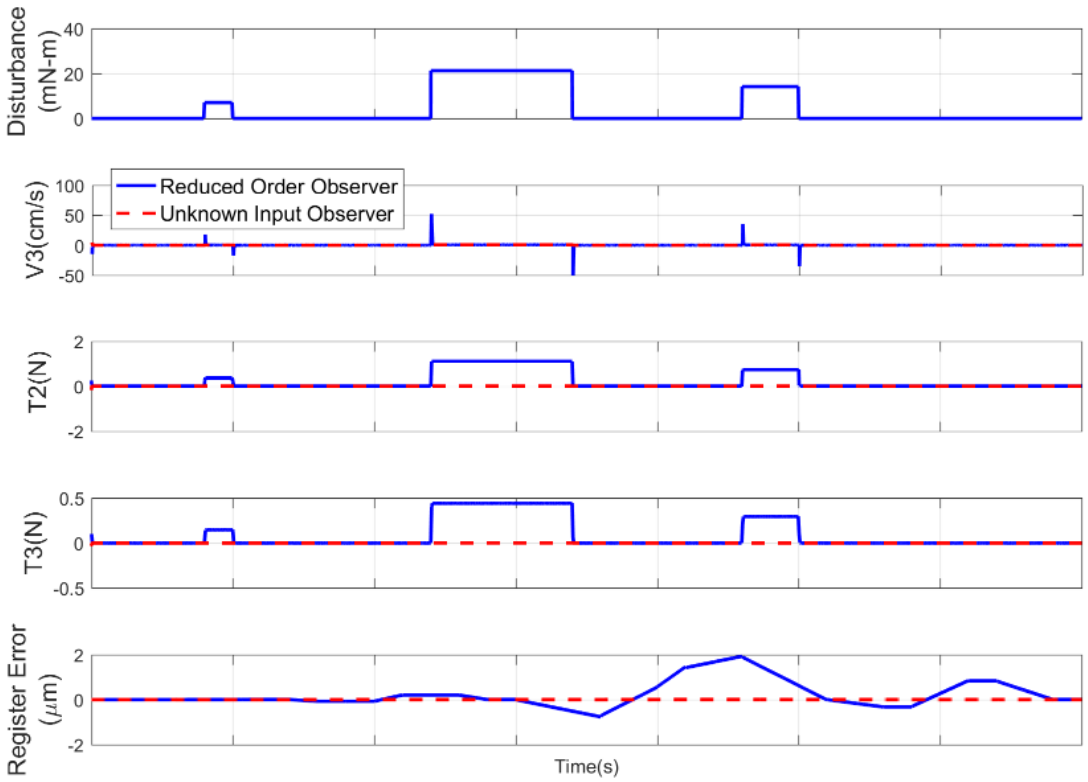

Figure 10. Comparison of the centralized MIMO controller with a reduced order observer and an unknown input observer

The unknown input observer is designed as described in Section 4.4. The input distribution variable, E, will be defined as follows:

$$\boldsymbol{E} = [\mathbf{0} \quad \mathbf{0} \quad \mathbf{1}] \tag{57}$$

This selection satisfies the necessary conditions and represents the expected disturbances to the roll-to-roll system. This indicates that disturbances are expected to enter the system through only on the rewind roller, even though input disturbance is present on all three driven rollers. Ideally, the input distribution *E* should be selected to reflect the actual

disturbances on the system. However, this will be different for each machine and a control designer will not always have an accurate disturbance model readily available. This simulation serves to show the performance of the observer even under poor assumptions. Note that the selection of E is based on the necessary condition of the unknown input observer. The goal is to evaluate the viability of the strategy even when the control designer does not know the disturbances exactly.

Figure 11 shows the results of the MIMO controller with the unknown input observer and compared to the reduced order observer with a 15% torque disturbance. The performance significantly improves and nearly tracks zero error for both state and registration error. In fact, the capabilities of this controller with the unknown input observer closely matches the results with full state feedback.

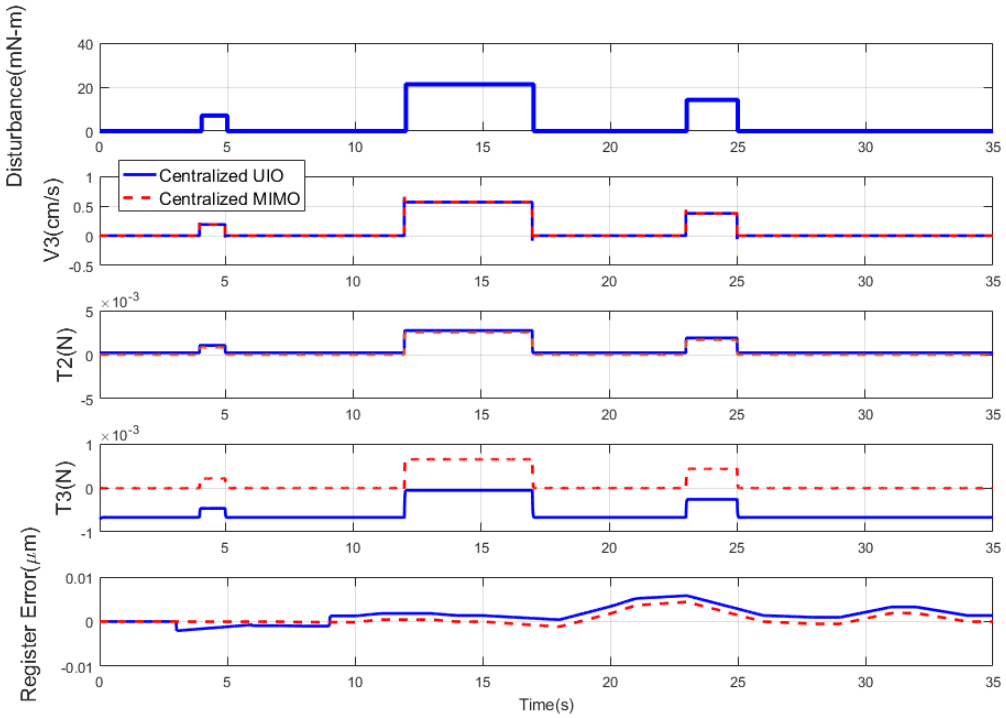

Figure 11. Comparison of centralized MIMO controller with full state feedback and an unknown input observer

In Figure 11, the observer performance has comparable performance to the full state feedback MIMO controller result. The unknown input observer achieves a peak registration error of 5.8 nm compared to the full state feedback result of 4.4 nm.

The unknown input observer has the best performance but there are limitations that must be kept in mind. The most fundamental assumption in this framework is the disturbance to the system is introduced at the input. Disturbances can occur from other sources, such as modeling uncertainty, measurement noise, or state disturbance. Note that there is an offset on *T3* in Figure 11. This can be explained by the fact that the input distribution *E* was wrongly assumed during the design phase. One of the principles behind the unknown input observer is the ability to not only estimate the state but also the disturbance. However, an incorrect input distribution model will lead to inaccurate disturbance estimation which results in state estimates not asymptotically converging. Essentially, measured velocity error has been attributed to disturbance rather than tension estimation error. Additionally, the theory is based on linear time invariant systems, but the simulation utilized the nonlinear plant model. While problematic from a theoretical perspective, the offset is small in comparison to the reference tension and registration error is within tolerance. The simulation was conducted under non-ideal conditions and assumptions to fully demonstrate the capabilities of the design. Thus, the proposed controller with unknown input observer can still have practical application.

Since the purpose of the observer is to replace tension load cells in the system, evaluation of the estimation error should be compared to measurement noise from a load cell. Many high precision instruments are available with a rated 0.3% of rated output [69]. For our simulation, a 50N reference tension would have a range of ±0.15N while Figure 10 shows an estimation error less than 0.001N.

There are still other important insights that can be gained from this simulation result. An accurate disturbance model will significantly improve control performance and state estimation even when the disturbance itself is an unknown. The assumption that disturbance occurs at the input is corroborated by the literature survey. Disturbances at

the driven rollers can include the motor, eccentric rollers, and velocity measurement error. These uncertainties will have a dominant effect on the overall system compared to disturbances during transport sections of the moving web. Despite inherent limitations, the unknown input observer has the best performance potential for observer based control designs and should be a priority for future work.

6.4 RESULTS AND DISCUSSION

The results presented in Section 6.1 - 6.3 only include a peak input disturbance of 15% equilibrium motor torque. Multiple simulations were conducted at various disturbance levels to create a more comprehensive data set for analysis. These results are shown in Table 4.

Max registration error (μm) for different peak torque disturbances					
Torque disturbance	1%	3%	5%	10%	15%
Decentralized SISO with full state feedback	0.0053	0.0164	0.0281	0.0598	0.0951
Centralized MIMO with full state feedback	2.56E-04	7.98E-04	0.0014	0.0028	0.0044
Centralized MIMO with reduced order observer	0.1209	0.3582	0.6026	1.2447	1.9305
Centralized MIMO with extended Kalman filter	0.1127	0.3439	0.5829	1.2148	1.8951
Centralized MIMO with unknown input observer	0.0021	0.0022	0.0027	0.0042	0.0058

Table 4. Summary of Registration Error

One nano-manufacturing technique, electron-beam lithography has been shown to print features under 10 nm, or 0.01 μm [70]. One of the motivations for this research is to meet these precision requirements so that technology developed by nanomanufacturing field can be applied to a roll-to-roll process.

Decentralized SISO with full state feedback is representative of typical control schemes for large scale roll-to-roll system. In fact, the decentralized controller would be

suitable for a wide variety of low precision applications. The drawback is that the control required full state feedback. Therefore, tension sensors would need to be placed in the system. Likewise, the state feedback is needed for the centralized MIMO controller. The difference is the centralized control provides significant improvement in minimizing the registration error.

The basic reduced order observer offers an easily implementable tension estimator at the expense of accuracy and performance. Even with a centralized MIMO framework, the reduced order observer performed the worst out of all the control schemes in this research. The second observer based control was the extended Kalman filter and the results did not improve significantly. The slight improvement was attributed to the nonlinear model and noise compensation but still fails to meet our control objective. The last control design, the unknown input observer, had the best performance out of all the observer based strategies.

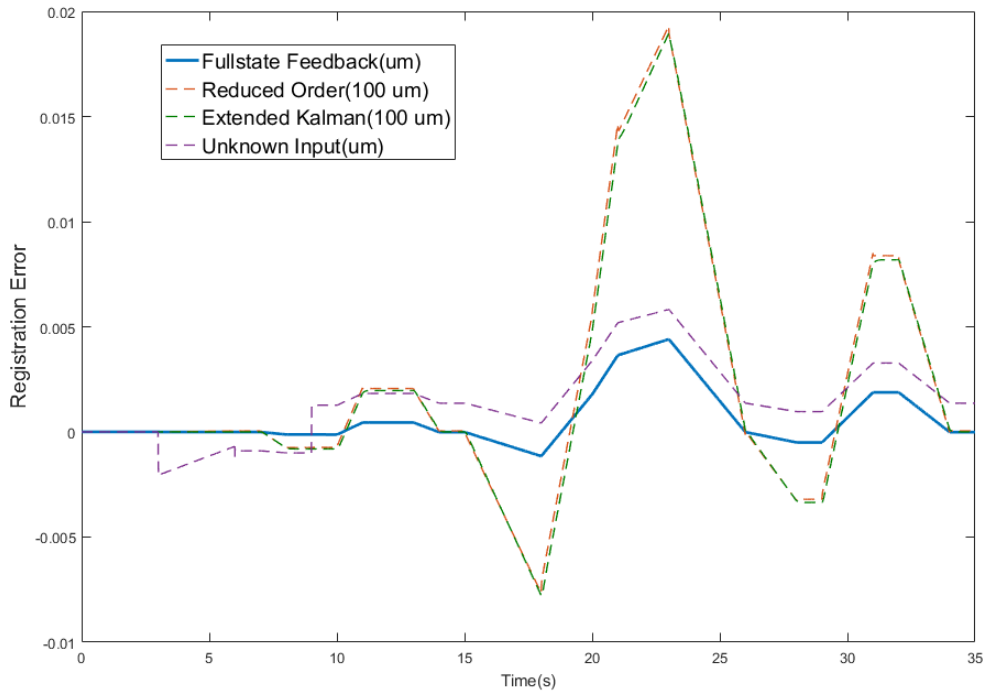

Figure 12 Comparison of centralized MIMO control with full state feedback and all observer-based tension feedback

The registration error results of the feedback and observer-based controllers under 15% torque disturbance are summarized in Figure 12. Note that the reduced order and extended Kalman filter data set were too large compared to the unknown input and full state feedback results and had to be scaled down by 100 times. Therefore, it is important to know that the performance of these two observers are much worse than appears in Figure 12. For the unknown input observer, the performance closely matched the full state feedback. The error deviated from zero at three seconds since the observer states were initialized far from actual values. The registration error was not corrected due to the estimation error described in Section 6.3.3.

One trend from Table 4 is the registration error scaled linearly with respect to torque disturbance, except for the unknown input disturbance. The error at 15%

disturbance is higher than at lower levels, but notice that at 1%, 3%, and 5%, the error seems to fall within a small range. We examine the relationship between magnitude of the disturbance with the magnitude of the state and registration error in the following.

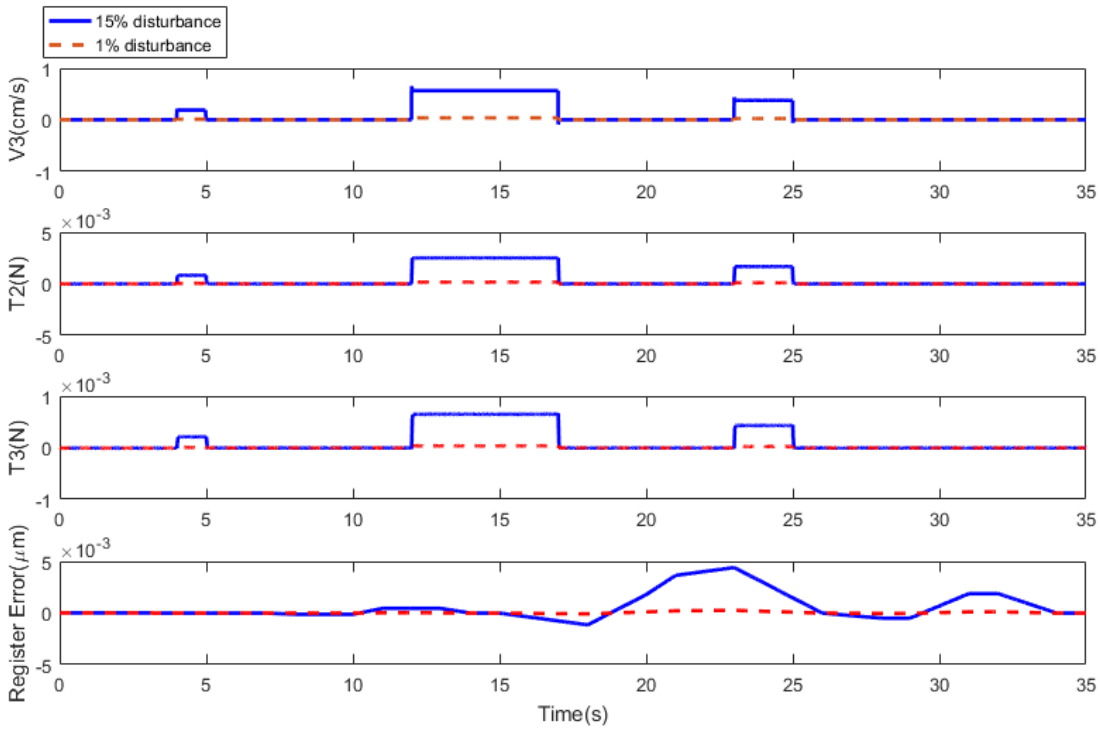

Figure 13. Performance of centralized MIMO full state feedback with 1% disturbance and with 15% disturbance

The results from Figure 13 show that the performance of the centralized MIMO control heavily depends on the level of disturbance. Across all the simulations presented in this thesis, the state errors and registration all seem to follow the same profile, but with different magnitudes. This seems to indicate that the control framework lacks a method of proportional disturbance compensation; for higher disturbance levels, the control action should be greater. Another fact is that the design is based on LQR and the weighting matrices had not been tuned for each of these simulations conditions. Even though the 15% result in Figure 13 appears drastically worse, note that this is still within the 10 nm tolerance identified in this thesis. Therefore, the control objective set forth in this

research has still been met; however, there is possibility for further improvements should the need arise in the future.

7 CONCLUSIONS

7.1 SUMMARY

In this paper, an observer based control methodology for minimizing registration error was presented. Modeling of the roll-to-roll system as well as a registration error model from literature was used in the control design. The control framework centered around selection of decentralized or centralized control strategy, as well as selection of appropriate tension observer, in order to maximize control performance.

The contribution of this thesis is a centralized MIMO control framework with tension observer that can meet the precision demands for flexible electronic fabrication using a roll-to-roll manufacturing process. The linear quadratic regulator from optimal control theory was formulated in order to minimize state and registration error. Both decentralized and centralized controllers were designed and simulated in order to compare performance. The centralized MIMO controller with full state feedback demonstrated significantly better tension and velocity reference tracking and smaller registration error compared to the decentralized scheme.

Second, three tension observers were designed and simulated to formulate a complete observer based centralized MIMO controller. The reduced order observer had an advantage in ease of implementation at the cost of worse tracking performance. The extended Kalman filter performed better by compensating for noise and nonlinearity, but still produced unacceptable performance. The reduced order observer and extended Kalman filter both failed to compensate for large input disturbances. The unknown input disturbance observer provided the best performance by modeling the disturbance as an unknown input in the state space model. Several assumptions and necessary conditions required for the unknown input disturbance observer made the formulation cumbersome and most difficult to implement compared to the other two observers.

Overall, a centralized MIMO controller with the unknown input observer demonstrated remarkable registration error minimization, well within the demands for high quality flexible electronic fabrication. The results from the decentralized controller and

other tension observers also provide valuable insights. In the simulation studies, all the results were under 2 μm. For many processes, this level of accuracy is sufficient and a simpler control design can be selected for ease of implementation.

7.2 FUTURE WORK

First, the centralized MIMO control design should be tested on an experimental platform to corroborate the simulation results. There are also multiple approaches to improving the controller proposed in this thesis. The unknown input observer can be improved with a better input disturbance distribution by using experimental data.

As for practical application, the framework should be extended to include multilayer registration error modeling. In multilayered registration, two or more printed features need to be aligned in the finished products, and error upstream can quickly propagate to downstream processes. The multiple layers add complexity to overall system and it is unclear if the centralized framework can handle the higher order system in real time.

State estimation for the roll-to-roll system has many potential areas of improvement. The proposed unknown input observer lacked methods for addressing modeling uncertainty and even introduced uncertainty in the input disturbance model when disturbance was in fact small or did not exist, causing a mismatch between the model and the system dynamics.

Ultimately, the main control objective is minimization of registration error. One main issue that needs to be addressed is the time delay component in the registration error model. By definition, the measurement of the error is time delayed: the difference between a reference and desired position is measured sometime after the reference point is selected. Furthermore, the time delay is variable based on the desired velocity. The delay was unaddressed in the proposed framework, hence the delay in the registration error could be seen in the results presented in this thesis. A control framework which addresses these time delay issues will significantly improve performance and warrants further investigation in the future.

Unless control hardware has significant improvements in computational power, decentralized control strategies will still be needed to reduce computational burden for real time control. The challenge in roll-to-roll manufacturing is designing a decentralized framework that can still meet registration error requirements.

Bibliography

[1] Energy, U. S. D. of, ed., 2015, “Quadrennial Technology Review 2015 Chapter 6K: Roll-to-Roll Processing.”

[2] Koc, H., Knittel, D., de Mathelin, M., and Abba, G., 2002, “Modeling and Robust Control of Winding Systems for Elastic Webs,” Ieee Trans. Control Syst. Technol., **10**(2), pp. 197–208.

[3] Kuhm, D., and Knittel, D., 2012, “New Mathematical Modelling and Simulation of an Industrial Accumulator for Elastic Webs,” Appl. Math. Model., **36**(9), pp. 4341–4355.

[4] Whitworth, D. P. D., and Harrison, M. C., 1983, “Tension Variations in Pliable Material in Production Machinery,” Appl. Math. Model., **7**(3), pp. 189–196.

[5] Seshadri, A., Raul, P. R., and Pagilla, P. R., 2014, “Analysis and Minimization of Interaction in Decentralized Control Systems With Application to Roll-to-Roll Manufacturing,” Ieee Trans. Control Syst. Technol., **22**(2), pp. 520–530.

[6] Lu, Y. W., and Pagilla, P. R., 2016, “A Nonlinear Tension Control Scheme for Web Transport through Heating Processes,” Proc. Asme 8th Annu. Dyn. Syst. Control Conf. 2015, Vol 2.

[7] Lu, Y. W., and Pagilla, P. R., 2014, “Adaptive Control of Web Tension in a Heat Transfer Section of a Roll-to-Roll Manufacturing Process Line,” 2014 Am. Control Conf.

[8] Lee, C. W., and Shin, K. H., 2005, “Strip Tension Control Considering the Temperature Change in Multi-Span Systems,” J. Mech. Sci. Technol., **19**(4), pp. 958–967.

[9] Vedrines, M., and Knittel, D., 2005, “An Improved Friction Sliding Model for Web Handling Systems. Application to the Controller Parametrization,” IFAC Proc., **38**(1), pp. 217–222.

[10] Shin, K. H., Jang, J. I., Kang, H. K., and Song, S. H., 2003, “Compensation Method for Tension Disturbance Due to an Unknown Roll Shape in a Web Transport System,” Ieee Trans. Ind. Appl., **39**(5), pp. 1422–1428.

[11] Branca, C., Pagilla, P. R., and Reid, K. N., 2013, “Governing Equations for Web Tension and Web Velocity in the Presence of Nonideal Rollers,” J. Dyn. Syst. Meas. Control. Asme, **135**(1).

[12] Xu, Y. L., 2009, “Modeling and LPV Control of Web Winding System with Sinusoidal Tension Disturbance,” Ccdc 2009 21st Chinese Control Decis. Conf. Vols 1-6, Proc., pp. 3815–3820.

[13] Young, G. E., and Reid, K. N., 1993, “Lateral and Longitudinal Dynamic Behavior and Control of Moving Webs,” J. Dyn. Syst. Meas. Control. Asme, **115**(2B), pp. 309–317.

[14] Shin, K. H., and Kwon, S. O., 2007, “The Effect of Tension on the Lateral Dynamics and Control of a Moving Web,” Ieee Trans. Ind. Appl., **43**(2), pp. 403–411.

[15] Guan, X., High, M. S., and Tree, D. A., 1995, “Viscoelastic Effects in Modeling Web Handling Systems: Steady-State Analysis,” J. Appl. Mech. Asme, **62**(4), pp. 908–914.

[16] Dwivedula, R. V, and Pagilla, P. R., 2013, “Effect of Backlash on Web Tension in Roll-to-Roll

Manufacturing Systems: Mathematical Model, Mitigation Method and Experimental Evaluation," 2013 Ieee Int. Conf. Control Appl., pp. 1087–1092.

[17] Wu, D. H., Chen, C., Yang, X. M., Li, X. S., and Huang, Y. M., 2014, "Optimization of Taper Winding Tension in Roll-to-Roll Web Systems," Text. Res. J., **84**(20), pp. 2175–2183.

[18] Kang, H., Lee, C., and Shin, K., 2010, "A Novel Cross Directional Register Modeling and Feedforward Control in Multi-Layer Roll-to-Roll Printing," J. Process Control, **20**(5), pp. 643–652.

[19] Lee, C., Lee, J., Kang, H., and Shin, K., 2009, "A Study on the Tension Estimator by Using Register Error in a Printing Section of Roll to Roll E-Printing Systems," J. Mech. Sci. Technol., **23**(1), pp. 212–220.

[20] Kang, H., and Baumann, R. R., 2014, "Mathematical Modeling and Simulations for Machine Directional Register in Hybrid Roll-to-Roll Printing Systems," Int. J. Precis. Eng. Manuf., **15**(10), pp. 2109–2116.

[21] Choi, K. H., Tran, T. T., Ganeshthangaraj, P., Lee, K. H., Nguyen, M. N., Jo, J. D., and Kim, D. S., 2010, "Web Register Control Algorithm for Roll-to-Roll System Based Printed Electronics," 2010 IEEE Int. Conf. Autom. Sci. Eng., pp. 867–872.

[22] Liu, S. H., Mei, X. S., Li, J., and Ma, L. E., 2013, "Machine Directional Register System Modeling for Shaft-Less Drive Gravure Printing Machines," Math. Probl. Eng.

[23] Liu, S. H., Yin, B. Z., Ma, L. E., Xu, H. W., and Zhu, G. S., 2016, "A Decoupling Control Strategy for Multilayer Register System in Printed Electronic Equipment," Math. Probl. Eng.

[24] Kang, H. K., Lee, C. W., and Shin, K. H., 2011, "Novel Modeling of Correlation between Two-Dimensional Registers in Large-Area Multilayered Roll-to-Roll Printed Electronics," Jpn. J. Appl. Phys., **50**(1).

[25] Pagilla, P. R., Dwivedula, R. V, and Siraskar, N. B., 2007, "A Decentralized Model Reference Adaptive Controller for Large-Scale Systems," Ieee-Asme Trans. Mechatronics, **12**(2), pp. 154–163.

[26] Raul, P. R., and Pagilla, P. R., 2015, "Design and Implementation of Adaptive PI Control Schemes for Web Tension Control in Roll-to-Roll (R2R) Manufacturing," Isa Trans., **56**, pp. 276–287.

[27] Nishida, T., Sakamoto, T., and Giannoccaro, N. I., 2013, "Self-Tuning PI Control Using Adaptive PSO of a Web Transport System with Overlapping Decentralized Control," Electr. Eng. Japan, **184**(1), pp. 56–65.

[28] Bouchiba, B., Hazzab, A., Glaoui, H., Med-Karim, F., Bousserhane, I. K., and Sicard, P., 2012, "Decentralized PI Controller for Multimotors Web Winding System," J. Autom. Mob. Robot. Intell. Syst., **6**(2), pp. 32–36.

[29] Nishida, T., Sakamoto, T., and Giannoccaro, N. I., 2013, "Self-Tuning PI Control Using Adaptive PSO of a Web Transport System with Overlapping Decentralized Control," Electr. Eng. Japan,

184(1), pp. 56–65.

[30] Shin, K. H., Kwon, S. O., Kim, S. H., and Song, S. H., 2003, "Feedforward Control of the Lateral Position of a Moving Web Using System Identification," 2003 Ieee Ind. Appl. Conf. Vols 1-3, pp. 345–351.

[31] Giannoccaro, N. I., Nishida, T., and Sakamoto, T., 2011, "Decentralized H∞ Based Control of a Web Transport System," IFAC Proc., **44**(1), pp. 8651–8656.

[32] Knittel, D., Arbogast, A., Vedrines, M., and Pagilla, P., 2006, "Decentralized Robust Control Strategies with Model Based Feedforward for Elastic Web Winding Systems," 2006 Am. Control Conf. Vols 1-12, **1**–**12**, pp. 1968–1975.

[33] Knittel, D., Vedrines, M., Henrion, D., and Pagilla, P., 2006, "Fixed-Order H(Infinity) Decentralized Control with Model Based Feedforward for Elastic Web Winding Systems," Conf. Rec. 2006 Ieee Ind. Appl. Conf. Forty-First Ias Annu. Meet. Vol 1-5, pp. 1315–1322.

[34] Benlatreche, A., Knittel, D., and Ostertag, E., 2008, "Robust Decentralised Control Strategies for Large-Scale Web Handling Systems," Control Eng. Pract., **16**(6), pp. 736–750.

[35] Knittel, D., Gigan, D., and Laroche, E., 2002, "Robust Decentralized Overlapping Control of Large Scale Winding Systems," Proc. 2002 Am. Control Conf. Vols 1-6, **1**–**6**, pp. 1805–1810.

[36] Knittel, D., Laroche, E., Gigan, D., and Koc, H., 2003, "Tension Control for Winding Systems with Two-Degrees-of-Freedom H-Infinity Controllers," Ieee Trans. Ind. Appl., **39**(1), pp. 113–120.

[37] Claveau, F., Chevrel, P., and Knittel, D., 2005, "A Two Degrees of Freedom H-2 Controller Design Methodology for Multi-Motors Web Handling System," ACC Proc. 2005 Am. Control Conf. Vols 1-7, pp. 1383–1388.

[38] Angermann, A., Aicher, M., and Schroder, D., 2000, "Time-Optimal Tension Control for Processing Plants with Continuous Moving Webs," Ias 2000 - Conf. Rec. 2000 Ieee Ind. Appl. Conf. Vols 1-5, pp. 3505–3511.

[39] Abjadi, N. R., Soltani, J., Askari, J., and Markadeh, G. R. A., 2009, "Nonlinear Sliding-Mode Control of a Multi-Motor Web-Winding System without Tension Sensor," Iet Control Theory Appl., **3**(4), pp. 419–427.

[40] Chen, C. L., Chang, K. M., and Chen, C. A. C. L., 2004, "Modeling and Control of a Web-Fed Machine," Appl. Math. Model., **28**(10), pp. 863–876.

[41] Yang, M., and Zhang, S. R., 2013, "Simulation and Research of Register Control System Based on Sliding Mode Variable Structure," 2013 25th Chinese Control Decis. Conf., pp. 514–519.

[42] Yun, S., Han, C., and Chung, J., 2001, "A Study on the Robust Control Algorithm for an Axially Moving Film," Ksme Int. J., **15**(9), pp. 1207–1216.

[43] Bouchiba, B., Hazzab, A., Glaoui, H., Med-Karim, F., Bousserhane, I. K., and Sicard, P., 2011, "Backstepping Control for Multi-Machine Web Winding System," J. Electr. Eng. Technol., **6**(1),

pp. 59–66.

[44] Choi, K. H., Tran, T. T., and Kim, D. S., 2011, “Back-Stepping Controller Based Web Tension Control for Roll-to-Roll Web Printed Electronics System,” J. Adv. Mech. Des. Syst. Manuf., **5**(1), pp. 7–21.

[45] Choi, K. H., Thanh, T. T., and Kim, D. S., 2009, “A Precise Control Algorithm for Single-Span Roll-to-Roll Web System Using the Back-Stepping Controller,” Isie 2009 Ieee Int. Symp. Ind. Electron., pp. 1692–1697.

[46] Tran, T. T., and Choi, K. H., 2014, “A Backstepping-Based Control Algorithm for Multi-Span Roll-to-Roll Web System,” Int. J. Adv. Manuf. Technol., **70**(1–4), pp. 45–61.

[47] Liu, S. H., Mei, X. S., Ma, L. E., You, H., and Li, Z., 2013, “Active Disturbance Rejection Decoupling Controller Design for Roll-to-Roll Printing Machines,” 2013 Int. Conf. Inf. Sci. Technol., pp. 111–116.

[48] Hou, Y., Gao, Z., Jiang, F., and Boulter, B. T., 2001, “Active Disturbance Rejection Control for Web Tension Regulation,” Proc. 40th Ieee Conf. Decis. Control. Vols 1-5, pp. 4974–4979.

[49] Zhou, W. K., and Gao, Z. Q., 2007, “An Active Disturbance Rejection Approach to Tension and Velocity Regulations in Web Processing Lines,” Proc. 2007 Ieee Conf. Control Appl. Vols 1-3, pp. 1178–1184.

[50] Lee, J., Seong, J., Park, J., Park, S., Lee, D., and Shin, K. H., 2015, “Register Control Algorithm for High Resolution Multilayer Printing in the Roll-to-Roll Process,” Mech. Syst. Signal Process., **60**–**61**, pp. 706–714.

[51] Seshadri, A., and Pagilla, P. R., 2013, “Decentralized Control of Print Registration in Roll-to-Roll Printing Presses,” Proc. Asme 2013 Dyn. Syst. Control Conf. (Dscc2013), Vol. 1.

[52] Chen, Z. H., He, J. J., Zheng, Y., Song, T., and Deng, Z. H., 2016, “An Optimized Feedforward Decoupling PD Register Control Method of Roll-to-Roll Web Printing Systems,” Ieee Trans. Autom. Sci. Eng., **13**(1), pp. 274–283.

[53] Cheng, C. W., Hsiao, C. H., Chuang, C. C., Chen, K. C., and Tseng, W. P., 2005, “Observer-Based Tension Feedback Control of Direct Drive Web Transport System,” 2005 IEEE Int. Conf. Mechatronics, pp. 745–750.

[54] Pagilla, P. R., King, E. O., Dreinhoefer, L. H., and Garimella, S. S., 2000, “Robust Observer-Based Control of an Aluminum Strip Processing Line,” Ieee Trans. Ind. Appl., **36**(3), pp. 865–870.

[55] Song, S. H., and Sul, S. K., 2000, “A New Tension Controller for Continuous Strip Processing Line,” Ieee Trans. Ind. Appl., **36**(2), pp. 633–639.

[56] Gassmann, V., and Knittel, D., 2008, “Tension Observers in Elastic Web Unwinder-Winder Systems,” Proc. Asme Int. Mech. Enginering Congr. Expo. 2007, Vol 9, Pts a-C, pp. 313–321.

[57] Lin, K. C., 2003, “Observer-Based Tension Feedback Control with Friction and Inertia

Compensation," Ieee Trans. Control Syst. Technol., **11**(1), pp. 109–118.

[58] Lin, K. C., 2002, "Frequency-Domain Design of Tension Observers and Feedback Controllers with Compensation," Iecon-2002 Proc. 2002 28th Annu. Conf. Ieee Ind. Electron. Soc. Vols 1-4, pp. 1600–1605.

[59] Gassmann, V., and Knittel, D., 2008, "H∞-Based PI-Observers for Web Tension Estimations in Industrial Unwinding-Winding Systems," IFAC Proc., **41**(2), pp. 1018–1023.

[60] Lynch, A. F., Bortoff, S. A., and Robenack, K., 2004, "Nonlinear Tension Observers for Web Machines," Automatica, **40**(9), pp. 1517–1524.

[61] Hailiang, H., Zhong, W., Xiaohong, N., and Jing, S., 2015, "Robust Decentralized Control of Web-Winding Systems without Tension Sensor," *Control Conference (CCC), 2015 34th Chinese*, pp. 8850–8854.

[62] Pagilla, P. R., Siraskar, N. B., and Dwivedula, R. V, 2007, "Decentralized Control of Web Processing Lines," Ieee Trans. Control Syst. Technol., **15**(1), pp. 106–117.

[63] Xin, H., "Design and Analysis for Roll-to-Roll Graphene Transfer."

[64] Skogestad, S., and Postlethwaite, I., 2007, *Multivariable Feedback Control: Analysis and Design*, Wiley New York.

[65] Luenberger, D. G., 1971, "An Introduction to Observers," IEEE Trans. Automat. Contr.

[66] Aldeen, M., and Trinh, H., 1994, "Observing a Subset of the States of Linear Systems," IEE Proc. - Control Theory Appl., **141**(3), pp. 137–144.

[67] Patton, R. J., Frank, P. M., and Clarke, R. N., eds., 1989, *Fault Diagnosis in Dynamic Systems: Theory and Application*, Prentice-Hall, Inc., Upper Saddle River, NJ, USA.

[68] Ogata, K., 1970, *Modern Control Engineering*.

[69] 2018, "DETERMINING LOAD CELL ACCURACY," (c), pp. 1–4 [Online]. Available: https://www.adminstrumentengineering.com.au/determining-load-cell-accuracy. [Accessed: 08-Dec-2018].

[70] Liddle, J. A., and Gallatin, G. M., 2016, "Nanomanufacturing: A Perspective," ACS Nano, **10**(3), pp. 2995–3014.